


**Please cite the Published Version**

Deswal, Sanjay, Chand Sharma, Milap, Saini, Rakesh, Chand, Pritam, Prakash, Satya, Kumar, Pawan, Barr, Iestyn , Umer Latief, Syed, Dalal, Padma and Bahuguna, IM (2023) Reconstruction of post-little ice age glacier recession in the Lahaul Himalaya, north-west India. *Geografiska Annaler Series A: Physical Geography*, 105 (1). pp. 1-26. ISSN 0435-3676

**DOI:** <https://doi.org/10.1080/04353676.2022.2148082>

**Publisher:** Taylor & Francis

**Version:** Accepted Version

**Downloaded from:** <https://e-space.mmu.ac.uk/631005/>

**Usage rights:**  [Creative Commons: Attribution-Noncommercial 4.0](https://creativecommons.org/licenses/by-nc/4.0/)

**Additional Information:** This is an Accepted Manuscript of an article published by Taylor & Francis in *Geografiska Annaler: Series A, Physical Geography* on 12th December 2022, available at: <http://www.tandfonline.com/10.1080/04353676.2022.2148082>. It is deposited under the terms of the Creative Commons Attribution-NonCommercial License (<http://creativecommons.org/licenses/by-nc/4.0/>), which permits non-commercial re-use, distribution, and reproduction in any medium, provided the original work is properly cited.

**Enquiries:**

If you have questions about this document, contact [openresearch@mmu.ac.uk](mailto:openresearch@mmu.ac.uk). Please include the URL of the record in e-space. If you believe that your, or a third party's rights have been compromised through this document please see our Take Down policy (available from <https://www.mmu.ac.uk/library/using-the-library/policies-and-guidelines>)

# Reconstruction of post-Little Ice Age glacier recession in the Lahaul Himalaya, north-west India

Sanjay Deswal<sup>a\*</sup>, Milap Chand Sharma<sup>b</sup>, Rakesh Saini<sup>c</sup>, Pritam Chand<sup>d</sup>, Satya Prakash<sup>e</sup>, Pawan Kumar<sup>f</sup>, Iestyn David Barr<sup>g</sup>, Syed Umer Latief<sup>h</sup>, Padma Dalal<sup>i</sup>, and I.M. Bahuguna<sup>j</sup>

<sup>a</sup> Department of Geography, Govt. College Chhara, District Jhajjar, Haryana, 124504, India

<sup>b</sup> Centre for the Study of Regional Development, Jawaharlal Nehru University, New Delhi, 110067, India

<sup>c</sup> Department of General & Applied Geography, Dr. Hari Singh Gour Central University, Sagar, 470003, India

<sup>d</sup> Department of Geography, School of Environment and Earth Sciences, Central University of Punjab, Bathinda, India

<sup>e</sup> Department of Geography, Govt. College Chowari, Chamba, Himachal Pradesh, India

<sup>f</sup> Department of Geography, Faculty of Physical Sciences, Chaudhary Bansi Lal University, Bhiwani, Haryana, India.

<sup>g</sup> School of Science and Environment, Manchester Metropolitan University, Manchester, United Kingdom

<sup>h</sup> Department of Geography, Amar Singh College Srinagar, J&K-190008 India

<sup>i</sup> Department of Geography, Government College Sampla (Rohtak), Haryana, India-124501

<sup>j</sup> Cryosphere Sciences Division, Space Application Centre, Ahmedabad, 380015, India

\*Corresponding Author, sdeswal.jnu@gmail.com

## Abstract

Understanding past glaciation and deglaciation is vital for assessing present-day glacier dynamics and response to climate change. We focus on reconstructing past glacier fluctuations in Lahaul, north-west India, a region located between arid Ladakh and the humid the Pir-Panjal range. We focus specifically on six glaciers in the Miyar and Thirot catchments of varying size, aspect, and debris cover. To reconstruct past terminus fluctuations of these glaciers, we used repeat terrestrial photography and historical archives as data sets and mapped the terminus positions and latero-terminal moraines in the field along with glacier terminus mapping from high to medium resolution satellite images (e.g. Corona, Hexagon, Landsat and LISS IV). Results show that since the LIA, all the studied glaciers have experienced terminus retreat and area loss, with average values of 1.46km and 0.9km<sup>2</sup> respectively. Precipitation data shows a statistically significant decreasing trend during the last century with increasing trend in annual average maximum ( $T_{max}$ ) and minimum ( $T_{min}$ ) temperature. This warming trend is more statistically significant for  $T_{min}$ . Although total ice loss at the six studied glaciers is considerable (5.48km<sup>2</sup>), this varies

both spatially (i.e., from glacier to glacier) and temporally. We attribute this variability to topographic controls such as glacier hypsometry and another non-climatic factor i.e. varying degree of debris cover.

**Keywords: Himalaya, Little Ice Age, Climate change, Glacier recession, Lahaul**

## **1. Introduction**

The Himalaya host the largest concentration of glaciers outside the polar regions and is considered as the water tower of south Asia (Immerzeel et al. 2010; Bolch et al. 2012). Most Himalayan glaciers have undergone continuous retreat and mass loss since the middle of the nineteenth century (Mayewski and Jeschke, 1979; Raina, 2009) and the rate of ice-loss during the 2000-2016 period was found to be double that in the 1975-2000 period (Maurer et al. 2019). This pattern of ice loss shows the accelerated impact of global warming due to the industrial revolution which is considered the reason for the termination of the Little Ice Age (LIA) (Vincent et al. 2005; Sedláček and Mysak 2009; Painter et al. 2013). The term LIA is used to refer to the most recent period of widespread climatic cooling, that typically occurred between 1400 and 1700 C.E., with greatest cooling over the extra-tropical Northern Hemisphere (Mann et al. 2009; Rowan 2017). Since glaciers in the Himalaya are influenced by two moisture sources, i.e., the Indian Summer Monsoon (ISM) and mid-latitude westerlies, their growth and decay vary spatially and temporally, producing intra-regional differences. This makes glacier fluctuations asynchronous between different parts of the Himalaya and when compared to other parts of the globe (Benn and Owen 1998). Therefore, timings of peak cooling and glacial maxima in the Himalaya during the LIA period also show intra-regional differences. Based on pollen data from Naychhudwari Bog in Himachal Pradesh, Chauhan (2006) analysed climate fluctuations during the last millennium, and found that from 1550 C.E. onwards, glaciers advanced as a result of a cold but dry climate, suggesting that temperature, rather than precipitation, controlled glacier behaviour. Rowan (2017) synthesized the

geochronology in the region and reported that glaciers in the Himalaya advanced during the late Holocene around 900 C.E. (based on 41 dates) and during the LIA between 1300 and 1600 C.E. (based on 25 dates). Geochemical analysis of sediments from Badanital lake (Garhwal Himalaya) by Kotlia and Joshi (2013) reveals evidence for comparatively warm conditions during 1080-1560 C.E. and cooler temperatures during 1560-1840 C.E.. This supports the idea of a relatively late LIA in the Western Himalaya, terminating during the mid-19<sup>th</sup> century. Recently, based on 635 years of reconstructed precipitation records (1383-2017) from tree rings, Singh et al. (2021) constrained the LIA between 1650-1850 in the western Himalayas. <sup>14</sup>C dates of archaeological sites from the same area also suggest a late LIA (Saini et al., 2019). Therefore, we take ~1850 to represent the LIA termination in our study.

Evidence of glacial advance during the LIA is often preserved in the form of fresh, sharp crested moraines, located within a few kilometres of present glacier termini (Sharma and Owen, 1996; Barnard et al., 2004; Owen et al., 2002, 1997, 1996; Scherler et al., 2010). Chand et al. (2017) reconstructed the fluctuations of Bara Shigri Glacier (in the Lahaul Himalaya, Figure 1) since the LIA maximum using a multi data integrated approach (MDIA) and revealed that at the LIA maximum the glacier extended 2.9 km beyond its present terminus position. However, terminus fluctuations vary from one glacier to another as dictated by various factors, including glacier geometry and hypsometry (Barr and Lovell 2014). Understanding post-LIA glacier retreat in the Himalaya is further complicated by the use of heterogeneous datasets. For example, there are various inventories of Himalayan glaciers viz. RGI (Randolph Glacier Inventory), but these differ in their estimates of total glacier number and glacier surface area (GLIMS, 2005; Pfeffer et al., 2014). With this backdrop, we map the present dimensions of all glaciers (109) in the Miyar-Thirot catchments (MTC) and undertake a detailed investigation of the post-LIA fluctuations of six of these (valley glaciers from the Lahaul Himalaya). Five of these glaciers (Miyar, Pimu, Menthosa, Tharang, and Uldhampu) lie within the Miyar basin, and one (Neelkanth) lies within the Thirot Nala sub-basin of Chandrabhaga ('Nala' is used for stream). According to the Geological Survey of India (GSI), there are eight glacierized fifth

order basins, viz. Kalnai, Marusudag, Bhut, Saichu, South Chenab, Miyar, Bhaga and Chandra in the Chenab, which is a fourth order basin (Special publication no. 63, 2001). Thiroi Nala, a sixth order basin, is a tributary of Chandrabhaga and joins it at village Thiroi (Figure 1). The purpose of this study is to contribute to an improved understanding of overall long-term glacial and climatic fluctuations in this region over the last century.

## **2. Regional Setting**

Located in the western Indian Himalaya, Lahaul is a major glaciated area, and the source region of River Chenab (Figure 1), which is known as Chandrabhaga in Lahaul. This region is in a transitional zone between the humid monsoonal south and arid north. The Pir-Panjal Range, to the south, largely restricts the north-eastward passage of monsoon rains, leaving Lahaul as a semi-arid region, influenced mostly by mid-latitude westerlies, commonly known as western disturbances. These westerlies typically result in precipitation, mainly snowfall, between December and April. The temperature reaches a maximum of 27.8°C in July and a minimum of -13.1°C in January. The mean annual air temperature (MAAT) is 7.6°C at the Keylong station (~ 3200 m a.s.l) with mean annual precipitation of 669.9 mm (Kaul and Thornton 2014). Mean annual rainfall from 1974 to 2005 was 241.5 mm and snowfall was 466.2 mm for another Indian meteorological department (IMD) station at Tandi (Rawat et al. 2009). Moreover, the IMD precipitation gridded data for the nearest grid that is within the Miyar Basin shows mean annual precipitation of 1270.7 mm during the past century (1901 to 2019) which is higher than at the Keylong and Tandi stations.

The study area represents a cross-section through the southern border of the High Himalayan Crystalline Zone (HHCZ) that crops-out as a large-scale dome structure (called the Gianbul dome) along the Miyar Valley-Gianbul Valley transect (Pognante et al. 1990; Vannay and Steck 1995; Robyr et al. 2002). The geological structure of the area is reflected in the drainage pattern, with igneous and high-grade metamorphic rock structure controlling drainage evolution, frequency and density. Smaller tributaries join main streams at an angle

of nearly 90° and form a trellised drainage pattern indicating strong geological control (Deswal et al. 2017).

The geochronology of former glaciation in the Miyar basin has been constrained previously using optically stimulated luminescence (OSL) and relative dating (Deswal et al. 2017). The oldest stage (MR-I) of glaciation/ice-advance in the basin has not been directly dated, but is inferred to be equivalent to the Chandra stage of Lahaul (Owen et al. 1996). A second stage (KH-II) has been chronologically constrained to 10-6 ka BP (OSL ages), making it equivalent to the early Holocene enhanced precipitation phase (Sarkar et al. 2000; Chakraborty et al. 2006). A recent glacial advance, named the Menthosa advance (M-III), is inferred to be equivalent to the LIA. The Chandra stage, represented by broad glacial trough and strath terraces, has not been dated in previous studies although it considerably predates Batal stage which was constrained with OSL dates of 43.4ka ±10.3ka BP (Owen et al. 1997) and later constrained in Zaskar Range to be ~78.0ka±12.3ka BP (Taylor and Mitchell 2000).(Table 4). Topographic maps are however highly useful if available for the glacier inventories prior to the satellite era, such as those used to prepare a glacial inventory in northern Norway (Weber et al., 2020).

1

#### 4.2 Pimu Glacier

Pimu glacier occupies the right bank tributary valley of the trunk Miyar valley with a northern aspect except at its terminus where it turns towards the north-east. It has two basins joining ~1 km upstream from the terminus, which lies at 4572 m a.s.l., and the base of the headwall altitude is 5163 m a.s.l. The contemporary ELA lies at 5090 m a.s.l. Pimu is a comparatively small glacier with a length of 4.7 km measured along the centreline of left basin and has a surface area of 5.52 km<sup>2</sup> comprising mainly clean ice and a small portion (~10%) of debris covered ice. A LIA lateral moraine (identified based on its sharp crested morphology) lies ~2.2 km from the contemporary terminus (Figure 5) indicating a recession rate of 13 m a<sup>-1</sup> since 1850 and an area loss of 1.13

km<sup>2</sup> (Table 2). The LIA position is also well represented in the 1871 GTS map (Figure 2a). Between 1971 and 2019, the glacier retreated ~349 m, corresponding to an average retreat rate of 7.3m a<sup>-1</sup> with an area loss of 123.52±2.64 m<sup>2</sup>(Table 3& 4). The rate of retreat was greatest between 1980 and 2002 (10.5m a<sup>-1</sup>) and appears to have slowed (to ~5.6 m a<sup>-1</sup>) more recently (Figure 5). This comparatively slow recent retreat rate potentially explains why field photographs show very little evidence of changing terminus configuration over recent years (Figure 5a & b).

#### 4.3 Menthosa Glacier

Menthosa is another major glacier with a south-easterly aspect and has a surface area of 5.81 km<sup>2</sup> (~25% of which is debris covered), and a centreline length of 4.3 km. Its contemporary terminus lies at 4400 m a.s.l. and the base of the headwall altitude is 5340 m a.s.l., while the contemporary ELA lies at 5180 m a.s.l. Since the LIA, Menthosa has retreated ~1.6 km (9.5 m a<sup>-1</sup>) and experienced an area loss of 0.66 km<sup>2</sup> (Table 2). Its LIA extent is marked by a set of sharp crested moraines free of vegetation or lichens (Figure 6a & b) that contrast with older (early Holocene) moraines near Urgos village (Deswal et al. 2017; Prakash et al. 2019) that are mapped in Figure 6e. The glacier boundary is slightly exaggerated in the 1871 GTS map (Figure 2a) and shows the terminus in an advanced position relative to the 1850 LIA moraine position, based on geomorphology (Figure 6e). Between 1850 and 1965 the glacier retreated ~1235 m, corresponding to an average retreat rate of 10.7 m a<sup>-1</sup>. Between 1965 and 2002, this retreat rate slowed to 5.1 m a<sup>-1</sup>, as the glacier retreated ~366 m (Figure 6, Table 3), but accelerated to 7.3 m a<sup>-1</sup> between 2002 and 2013 (Figure 3). A similar rate of retreat (5.9±0.4 m a<sup>-1</sup>) between 1965-2016 has been reported in a recent study (Prakash et al. 2021). The most recent retreat phase (between 2013 and 2019) was the most rapid of all (i.e., ~16 m a<sup>-1</sup>). This rapid recent retreat is clearly demonstrated in field photographs of the glacier terminus, captured in 2006 and 2016 (Figure 6 a & b). Overall loss of frontal area between 1965 to 2019 stands at 104.91 m<sup>2</sup> (Table 4).

Fluctuations of Menthosa glacier have created a spectacular assemblage of landforms. Similar to Pimu glacier, there are two basins of the Menthosa glacier. Left basin joins the major right-side basin from such an angle that there formed a long narrow deglaciated valley between the valley wall and the left lateral moraine of the glacier. Such valleys are commonly called ablation valleys as they exist along the ablation zone of the glacier. Benn and Evans, (2014) have referred such valleys as valley side depressions as they formed due to the deposition of debris along the valley wall. (Figure 6e). Within the ablation valley, there are three successive terminal moraines that are not dated with absolute ages but are most likely older than the LIA, given their stability and vegetation growth (Figure 6d). These terminal moraines are likely to have been deposited by small glaciers that are presently restricted to their respective cirques.

#### 4.4 Tharang Glacier

Tharang glacier lies in a left bank tributary valley with a north-west aspect. It has a total length of 4.3 km and surface area of 5.37 km<sup>2</sup>, with negligible debris cover. Its terminus altitude is 4507 m a.s.l. and the headwall altitude is 5636 m a.s.l., with a contemporary ELA at 5500 m a.s.l. Tharang Nala (stream) joins the river Miyar after flowing for 4.2 km from Tharang glacier's terminus. At the confluence of the Tharang and Miyar streams, an impressive sequence of end moraines (Figure 7c) deposited during the early Holocene are dated to 8-6 ka OSL ages (Deswal et al. 2017). The LIA extent of Tharang glacier is well preserved by sharp crested lateral moraines (Figure 2d and Figure 7a & b) and the 1871 terminus position is visible in the GTS map (Figure 2a). A former tributary glacier mapped in Figure 7c is shown to be joined to Tharang glacier in the GTS map of Figure 2a. At the Holocene end-moraine complex of Tharang glacier, there is also archaeological evidence that suggests human habitation within/upon these moraines during the 1300-1700 CE period (Saini et al. 2019). This indicates that 1300-1700 was a warmer period, constraining the LIA to the 19<sup>th</sup> century in this part of the

Himalayas. Since the LIA, Tharang glacier has retreated  $\sim 2.3$  km, at an average rate of  $\sim 14.2$  m  $a^{-1}$ . Between 1971 and 2002, the glacier retreated 145 m, averaging 4.7 m  $a^{-1}$  (Table 3). Between 2002 and 2013, the rate of recession increased dramatically, to 29.4 m  $a^{-1}$  (total retreat of 323 m), before slowing again, to 3.2 m  $a^{-1}$  (total retreat of 19 m) between 2013 and 2019 (Figure 3). Overall area loss between 1971 and 2019 stands at  $212.11 \pm 4.83$  m<sup>2</sup> (Table 4). a

#### 4.5 Uldhampu Glacier

Uldhampu glacier lies in adjoining basin of Tharang with a similar north-west aspect and a length of 6 km with a surface area of 5.86 km<sup>2</sup> ( $\sim 41\%$  of which is debris covered). Its terminus altitude is 4530 m a.s.l. and the base of the headwall lies at 5055 m a.s.l., while the contemporary ELA lies at 4990 m a.s.l. It has retreated  $\sim 1.1$  km ( $6.5$  m  $a^{-1}$ ) and experienced an area loss of 0.77 km<sup>2</sup> since the LIA (Table 2). Between 1971 and 2019, retreating Uldhampu glacier has vacated an area of  $245.36 \pm 3.78$  m<sup>2</sup> (Table 4). Between 1971 and 2002, the glacier experienced rapid retreat ( $16.2$  m  $a^{-1}$ ) but slowed considerably between 2002 and 2013 ( $1.7$  m  $a^{-1}$ ), before accelerating slightly (to  $4.0$  m  $a^{-1}$ ) between 2013 and 2019 (Table 3, Figure 3). This comparatively limited retreat in recent decades is illustrated in the geomorphological map (Figure 8b).

#### 4.6 Neelkanth Glacier

Neelkanth glacier is the main trunk glacier in the Thiroth Nala catchment, a tributary of the Chandrabhaga River adjoining the Miyar catchment. This glacier is 7.2 km in length along the centreline and has a surface area of 6.27 km<sup>2</sup> ( $\sim 33\%$  of which is debris covered). Its contemporary terminus lies at 4300 m a.s.l. and the base of the headwall is 5613 m a.s.l. with an ELA at 4940 m a.s.l. There is a moraine dammed lake between a lateral moraine and right-side valley wall at an elevation of 4500 m a.s.l. Detailed geomorphology and lake bathymetry is discussed in Deswal et al. (2020). There is a relationship between lake dam stability and recession of the glacier, as the receding glacier may cause instability to the dam and eventually trigger a lake outburst. This glacier was not mapped correctly in the GTS

map of 1871 (Figure 2a), so former glacier extents rely on the geomorphological record. In the glacier fore-field, there is an unambiguous sequence of Early Holocene and LIA moraines (Figure 9a & b). Since the LIA, the glacier has retreated  $\sim 1.3$  km from these moraines, corresponding to an average retreat rate of  $7.4 \text{ m a}^{-1}$ . Over recent years, this retreat rate has remained reasonably constant. For example, for the 1989-2002, 2002-2013, and 2013-2019 periods the average retreat rate was  $9.3 \text{ m a}^{-1}$ ,  $4.1 \text{ m a}^{-1}$ , and  $9.1 \text{ m a}^{-1}$ , respectively (Table 3, Figure 3).

## 5. Discussion

All six glaciers investigated in this study show evidence for continual terminus retreat and surface lowering since the LIA. This pattern is consistent with many other areas of the Himalaya and elsewhere globally (Mayewski and Jeschke 1979; Dobhal et al. 2004; Kulkarni et al. 2005; Granshaw and Fountain 2006; Kulkarni et al. 2006; Kulkarni et al. 2007; Bolch et al. 2008; Raina 2009; Bhambri et al. 2011; Schmidt, S. and Nusser 2012; Bolch et al. 2012; Pan et al. 2012; Chand and Sharma 2015a; Racoviteanu et al. 2015; Cook et al. 2016; Chand et al. 2017; Das and Sharma 2019). However, despite this overall trend, there is also evidence for inter-glacier and temporal variability in the retreat rates of the six glaciers considered here. Much of the variability in overall retreat rates since the LIA (ranging from  $5.3$  to  $13.6 \text{ m a}^{-1}$ ) likely results from differences in topography, local climate, and glacier hypsometry. The temporal variability in retreat rates may also reflect these local controls, since there are notable differences between glaciers. For example, since 1965, some (e.g., Pimu and Uldhampu) show a general reduction in retreat rates towards the present (Figure 3). Others (e.g., Miyar, Tharang, and Neelkanth) show variability, but no clear temporal trend in retreat rates, while Menthosa glacier shows evidence for increasing retreat rates towards the present (Figure 3). Despite these differences between glaciers, overall there is some (minor) evidence for slowing retreat rates towards the present. For example, between the LIA and 2019, the mean retreat rate for all six glaciers is  $9.3 \text{ m a}^{-1}$ . In the past two decades, this rate has slowed slightly, i.e.,  $9.2 \text{ m a}^{-1}$  between 2002 and 2013, and  $8.4 \text{ m a}^{-1}$  between 2013 and

2019. These overall retreat rates are slightly slower than observed in some other studies. For instance, Samudari tapu glacier in the Lahaul Himalaya (Figure 1) has a reported retreat rate of  $15.5 \text{ m a}^{-1}$  (a total distance of 588 m) between 1963 and 2001 (Shukla et al. 2009). However, particularly slow retreat rates have been reported in other studies in the region. For example, North of the present study area, in the Kang-Yatze massif of Zaskar, Schmidt and Nusser, (2012) reported average retreat rates of  $3 \text{ m a}^{-1}$  between 1969 and 2010. Similarly, south of our study area, in the Ravi basin, Chand and Sharma (2015a) reported slower retreat rates ( $4.7 \pm 4.1\%$ ) based on Corona and other high resolution data sets during the past four decades (i.e. 1971-2010/13).

### 5.1 Climatic controls on recent glacier retreat patterns

IMD gridded data based inter-annual climate trends were analysed using z statistics, linear regression, and the Theil Sen's method. A positive z-statistic value indicates an increasing trend in precipitation, whereas a negative z-statistic value indicates a decreasing trend. The annual precipitation ( $P_{avg}$ ) for the nearest cell of IMD gridded data shows a significant decreasing trend since 1900, with some cyclic drifts. Figure 10 shows the rainfall anomaly index and the five-year moving average which gives a representation of the temporal changes in precipitation. The IMD gridded precipitation data shows a statistically significant decreasing ( $z = -4.43$  and  $p \text{ value} < 0.01$ ) trend in overall precipitation in this region and particularly from the 1960s onwards. The Pettitt's test also identifies the change point for annual precipitation in 1959, which is statistically significant at a 95 percent confidence level. Precipitation trends also show seasonal differences for instance, the monsoonal (JJA) ( $z = -4.55$  and  $p \text{ value} = 0.0000054$ ) and post-monsoonal (SON) ( $z = -1.95$  and  $p \text{ value} = 0.05$ ) precipitation show statistically significant decreasing trends since 1951. Analysis of variability in precipitation patterns using coefficient of variation (CV) for 1901–2019 for the upper Chenab basin shows annual precipitation variability (Figure 11b). The variation is higher for the Miyar basin when compared to the Bhaga and Chandra basins of the upper Chenab. Regions with higher annual variability in precipitation are more susceptible to floods and

droughts (Pandey and Ramasastri 2002; Turkes, 1996). The rainfall anomaly index shows a continuous drought (during all seasons) since the 1960s for the IMD gridded dataset within the Miyar basin. Such conditions are likely to have limited glacial accumulation, and thereby promoted glacier retreat during this period. This may (at least partly) explain glacier retreat rates during the past half-century in the basin. The annual average maximum ( $T_{\max}$ ) and minimum ( $T_{\min}$ ) temperature for the nearest grid cell of the IMD data show significant warming trends during the past half-century (1951-2019), with some cyclic patterns. This warming trend is more statistically significant for  $T_{\min}$  ( $z = 2.45$  and  $p$  value = 0.014). The Sen's slope estimator further supports these findings and suggests an  $T_{\min}$  increase of  $0.51^{\circ}\text{C}$  at the rate of  $0.008^{\circ}\text{C a}^{-1}$  from 1951 to 2019. The post-monsoon period and winter months show a statistically significant increasing average  $T_{\min}$  of  $0.84^{\circ}\text{C}$  and  $0.51^{\circ}\text{C}$  respectively from 1951 to 2019.  $T_{\max}$  also shows an increase of  $0.34^{\circ}\text{C}$  at a rate of  $0.005^{\circ}\text{C a}^{-1}$  from 1951 to 2019, and similar trends are observed for all seasons except the monsoon which shows a statistically insignificant decreasing trend of  $0.05^{\circ}\text{C}$  at a rate of  $0.001^{\circ}\text{C a}^{-1}$  from 1951 to 2019. Overall, the IMD gridded dataset shows a decreasing precipitation trend for the past century (1901–2019), whereas annual temperature shows an increasing trend, which is slightly more notable for  $T_{\min}$  than  $T_{\max}$  and during winter months as compared to other seasons. Based on IMD gridded data, Bhutiyani (2016) reveals that the warming trend in winter has led to a declining snowfall contribution to total precipitation. Thus, it seems that the reported decrease in snowfall and overall precipitation coupled with the observed increasing temperature trends are probably the main drivers of observed changes in glacier extent in the present study over recent decades.

## 5.2 Topographic factors

In addition to the moisture supply, mountain glaciers are also controlled by topography and valley geometry that makes their response to climate change very complex, resulting into variation in ELAs from one glacier to the other (Owen and Benn 2005). Therefore, reconstruction of palaeo ELAs based on former glacier extents is problematic in high altitude

environments such as the Himalaya (Owen et al. 2005; Kleman et al. 2006; Thomas 2013; Barr and Lovell 2014). The ELA is largely controlled by the local climate, the inter-glacier variation of terminus fluctuation is however mainly determined by the topography. The use of hypsometric curves (area in relation to elevation) has widely been used to infer glacier regimes and their response time to climate change (Furbish and Andrews 1984; Oerlemans 1989; Raper and Braithwaite 2009; McGrath et al. 2017). Raper and Braithwaite, (2006) argued that median altitude of the glacier (which divide the glacier in two equal halves) coincide with the mid elevation of the glacier and the ELA for steady-state glaciers (when the glacier is in equilibrium) and the area-altitude distribution plots are triangular and symmetrical about the ELA (Figure 11). Area-altitude distribution of the studied glaciers show the effect of valley geometry and factors viz. debris cover on the terminus position as the plots are asymmetric (Figure 12). Pimu and Tharang glaciers with lowest debris cover among all studied glaciers (10.3% and 0 respectively), are tending towards symmetrical area-altitude plots and are bound to be retreated further at terminus. All other glaciers with significant debris cover (Table 2) are showing asymmetric plots which is an indication that debris cover in ablation zones is protecting these glaciers from rapid retreat due to the insulating effect. Patel et al. (2018) also highlighted similar results regarding the effect of debris cover on glacier retreat in the Miyar basin. The slow retreat due to debris cover is however, resulting into glacier thinning ever since the termination of LIA which is conspicuous from the LIA moraines (Figure 2 c & d) as reported from other regions also (Bolch et al. 2008; Pratap et al. 2015). Glacier size is another important factor, along with debris cover, that is responsible for varying terminus fluctuations. Miyar, the largest glacier (Table 2) among all studied glaciers has recorded the lowest linear retreat (0.9km) of the terminus with the largest area vacated (1.14km<sup>2</sup>).

Further, the difference between the median elevation of the glacier ( $Z_{med}$ ) and the midpoint elevation or the half range of the glacier ( $Z_{mid}$ ) shows the effect of valley geometry on the distribution of glacier area across the altitudinal range (Table 5, Figure 11). The

Hypsometric Index (HI) is one such method which highlights the valley geometry and HI of the studied glaciers (Table 5) and this has been calculated using the method of McGrath et al., (2017):

where  $H_{\max}$  and  $H_{\min}$  are the maximum and minimum glacier elevations above sea level while  $H_{\text{med}}$  is median elevation of the glacier. McGrath et al., (2017) further added that if  $0 < HI < 1$  then  $HI = -1/HI$  and grouped the glaciers into very top heavy ( $< -1.5$ ), top heavy ( $-1.5 < HI < -1.2$ ), equidimensional ( $-1.2 < HI < 1.2$ ), bottom heavy ( $1.2 < HI < 1.5$ ) and very bottom-heavy glaciers ( $> 1.5$ ). The Miyar glacier with HI of -1.0 is categorized as equidimensional with a little difference between  $Z_{\text{mid}}$  and  $Z_{\text{med}}$  while the Tharang glacier is found to be very top heavy with HI of -1.7 (Table 5). All other glaciers fall under the category of very bottom-heavy meaning thereby these glaciers occupy less area above mid-elevation (Table 5). The significance of HI method lies in its simplicity and explicability in determining the role of valley geometry.

The control of valley geometry over the glacier ice distribution across the altitudinal range and the fluctuation at the terminus is also conspicuous when we look at the LIA positions of the studied glaciers in relation to the early Holocene moraine positions. The early Holocene positions of Menthosa, Tharang and Uldhampu glaciers are extended up to ~4km from the respective LIA positions (Figures 6, 7 & 8 respectively). Notably all these glaciers have ~17° of average slope (Table 5). Interestingly, the Neelkanth glacier with a similar slope almost approached its Holocene position during the LIA (Figure 9). Similarly, Miyar glacier with a gentle average slope of 12.2° (Table 5) terminated just 0.5km before its Holocene position (Figure 4). Therefore, valley geometry and various glacier characteristics viz. debris cover, slope, aspect etc. play an important role in determining the inter-glacier variation in a region.

## 6. Conclusions

Little Ice Age (LIA) glacier advance in the western Himalayas has been linked to a 18<sup>th</sup> century cooling episode that terminated ~1850 C.E. The present study provides a reconstruction of post LIA glacier fluctuations in the semi-arid Lahaul Himalaya region of north-west India, where precipitation is dominated by mid latitude westerlies. A multi-data integrative analysis (MDIA) technique was implemented, which includes the use of repeat terrestrial photographs, historical archives, mapping from high to medium spatial resolution satellite images (Corona, Hexagon, Landsat and LISS IV) and field-based monitoring and verification. Six glaciers were studied, each from the Miyar and Thirot catchments (MTC) of the Lahaul Himalaya. These glaciers vary in size, aspect, and debris cover (among other characteristics), and are found to have experienced continuous terminus retreat and area loss since the LIA. The extent of terminus retreat and surface area loss between the LIA and 2019 is 0.9 km (Miyar Glacier), 2.3 km (Tharang Glacier), 0.66 km<sup>2</sup> (Menthosa Glacier) and 1.14 km<sup>2</sup> (Miyar Glacier). There is no consistent (inter-glacier) temporal pattern in glacier retreat rates, though some show evidence of accelerated retreat rates over recent years. This temporal and inter-glacier variability in the extent and rate of glacier retreat is likely driven by the combined influence of climate (air temperature and precipitation) and topography.

## **Acknowledgement**

We are grateful to SERB/DST Govt. of India for providing financial support (Ref. SERB/F/1731/2014-15 dated 16-06-2014).

## **References**

Agrawal A, Sharma AR, Tayal S. 2014. Assessment of regional climatic changes in the Eastern Himalayan region: a study using multi-satellite remote sensing data set. *Environ Monit Assess.* 186:6521–6536. <https://doi.org/10.1007/s10661-014-3871-x>

Azam MF, Wagnon P, Vincent C, Ramanathan A, Linda A, Singh VB. 2014. Reconstruction of the annual mass balance of Chhota Shigri glacier, Western Himalaya, India, since 1969. *Ann Glaciol.* 55(66):69–80. <https://doi.org/10.3189/2014AoG66A104>

Barnard PL, Owen LA, Sharma MC, Finkel RC. 2004. Late Quaternary (Holocene) landscape evolution of a monsoon-influenced high Himalayan valley, Gori Ganga, Nanda Devi, NE Garhwal. *Geomorphology.* 61(1–2):91–110. <https://doi.org/10.1016/j.geomorph.2003.12.002>

Barr ID, Lovell H. 2014. A review of topographic controls on moraine distribution. *Geomorphology* [Internet]. 226:44–64. <https://doi.org/10.1016/j.geomorph.2014.07.030>

Benn D, Evans DJA. 2014. *Glaciers and glaciation*. [place unknown]: Routledge.

Benn DI, Owen LA. 1998. The role of the Indian summer monsoon and the mid-latitude westerlies in Himalayan glaciation: review and speculative discussion. *J Geol Soc London* [Internet]. 155(2):353–363. <https://doi.org/10.1144/gsjgs.155.2.0353>

Benn DI, Owen LA, Osmaston HA, Seltzer GO, Porter SC, Mark B. 2005. Reconstruction of equilibrium-line altitudes for tropical and sub-tropical glaciers. *Quat Int* [Internet]. 138–139:8–21. <https://doi.org/10.1016/j.quaint.2005.02.003>

Bhambri R., Bolch T, Chaujar RK. 2011. Mapping of debris-covered glaciers in the Garhwal Himalayas using ASTER DEMs and thermal data. *Int J Remote Sens* [Internet]. 32(23):8095–8119. <https://doi.org/10.1080/01431161.2010.532821>

Bhambri Rakesh, Bolch T, Chaujar RK, Kulshreshtha SC. 2011. Glacier changes in the Garhwal Himalaya , India , from 1968 to 2006 based on remote sensing. *J Glaciol.* 57(203):543–556.

Bhutiyan MR. 2016. Spatial and temporal variability of climate change in high-altitude regions of NW Himalayas. *Clim Chang glacier response, Veg Dyn Himalaya Springer, Cham* [https://doi.org/10.1007/978-3-319-28977-9\\_5](https://doi.org/10.1007/978-3-319-28977-9_5).

Bolch T, Buchroithner M, Pieczonka T, Kunert A. 2008. Planimetric and volumetric glacier changes in the Khumbu Himal, Nepal, since 1962 using Corona, Landsat TM and ASTER data. *J Glaciol* [Internet]. 54(187):592–600. <https://doi.org/10.3189/002214308786570782>

Bolch T, Kulkarni A, Kaab A, Huggel C, Paul F, Cogley JG, Frey H, Kargel JS, Fujita K, Scheel M, et al. 2012. The State and Fate of Himalayan Glaciers. *Science* (80- ) [Internet]. 336(6079):310–314. <https://doi.org/10.1126/science.1215828>

Bolch T, Menounos B, Wheate R. 2010. Landsat-based inventory of glaciers in western Canada, 1985–2005. *Remote Sens Environ* [Internet]. 114(1):127–137. <https://doi.org/10.1016/j.rse.2009.08.015>

Chakraborty S, Bhattacharya SK, Ranhotra PS, Bhattacharyya A, Bhushan R. 2006. Palaeoclimatic scenario during Holocene around Sangla valley, Kinnaur northwest Himalaya based on multi proxy records. *Curr Sci*. 91(6).

Chand P, Sharma MC. 2015a. Frontal changes in the Manimahesh and Tal Glaciers in the Ravi basin, Himachal Pradesh, northwestern Himalaya (India), between 1971 and 2013. *Int J Remote Sens* [Internet]. 36(16):4095–4113. <https://doi.org/10.1080/01431161.2015.1074300>

Chand P, Sharma MC. 2015b. Glacier changes in the Ravi basin, north-western Himalaya (India) during the last four decades (1971–2010/13). *Glob Planet Change* [Internet]. 135:133–147. <https://doi.org/10.1016/j.gloplacha.2015.10.013>

Chand P, Sharma MC, Bhambri R, Sangewar C V, Juyal N. 2017. Reconstructing the pattern of the Bara Shigri Glacier fluctuation since the end of the Little Ice Age, Chandra valley, north-western Himalaya. *Prog Phys Geogr* [Internet].:030913331772801. <https://doi.org/10.1177/0309133317728017>

Chandler BMP, Lovell H, Boston CM, Lukas S, Barr ID, Benediktsson ÍÖ, Benn DI, Clark CD, Darvill CM, Evans DJA. 2018. Glacial geomorphological mapping: A review of approaches and frameworks for best practice. *Earth-Science Rev.* 185:806–846.

Chauhan MS. 2006. Late Holocene vegetation and climate change in the alpine belt of Himachal Pradesh. *Curr Sci.* 91(11):1562–1567.

Cook SJ, Kougkoulos I, Edwards LA, Dortch J, Hoffmann D. 2016. Glacier change and glacial lake outburst flood risk in the Bolivian Andes. *Cryosphere.* 10(5). <https://doi.org/10.5194/tc-10-2399-2016>

Das S, Sharma MC. 2019. Glacier changes between 1971 and 2016 in the Jankar Chhu Watershed, Lahaul Himalaya, India. *J Glaciol* [Internet]. 65(249):13–28. <https://doi.org/10.1017/jog.2018.77>

Deswal S, Sharma M, Saini R, Chand P, Juyal N, Singh I, Srivastava P, Ajai, Bahuguna IM. 2017. Late Holocene Glacier Dynamics in the Miyar Basin, Lahaul Himalaya, India. *Geosciences* [Internet]. 7(3):64. <https://doi.org/10.3390/geosciences7030064>

Deswal S, Sharma MC, Saini R, Dalal P, Kumar P. 2020. Preliminary results of hybrid bathymetry and GLOF risk assessment for Neelkanth lake, Lahaul Himalaya, India. *Curr Sci.* 119(9):1555.

Dobhal DP, Gergan JT, Thayyen RJ. 2004. Recession and morphogeometrical changes of Dokriani glacier ( 1962 – 1995 ) Garhwal Himalaya , India. *Curr Sci.* 86(5).

Frey H, Paul F, Strozzi T. 2012. Compilation of a glacier inventory for the western Himalayas from satellite data: methods, challenges, and results. *Remote Sens Environ* [Internet]. 124:832–843. <https://doi.org/10.1016/j.rse.2012.06.020>

Furbish, D.J. and Andrews JT. 1984. The use of hypsometry to indicate long-term stability and response of valley glaciers to changes in mass transfer. *J Glaciol.* 30(105):199–211.

GLIMS, National Snow IDC. 2005. GLIMS Glacier Database. [Himalaya], updated 2012. Natl Snow Ice Data Center, Boulder, CO, USA [Internet]. <http://dx.doi.org/10.7265/N5V98602>

Granshaw FD, Fountain AG. 2006. Glacier change ( 1958 – 1998 ) in the North Cascades National Park Complex, Washington, USA. *J Glaciol.* 52(177):251–256.

Hall DK, Bayr KJ, Schöner W, Bindschadler RA, Chien JYL. 2003. Consideration of the errors inherent in mapping historical glacier positions in Austria from the ground and space (1893-2001). *Remote Sens Environ.* 86(4):566–577.

Immerzeel WW, van Beek LPH, Bierkens MFP. 2010. Climate change will affect the Asian water towers. *Science* (80- ). 328(5984):1382–1385. <https://doi.org/10.1126/science.1183188>

Kaul V, Thornton TF. 2014. Resilience and adaptation to extremes in a changing Himalayan environment. *Reg Environ Chang* [Internet]. 14(2):683–698. <https://doi.org/10.1007/s10113-013-0526-3>

Kendall MG. 1970. Rank correlation methods. 4th ed. [place unknown]: Charles Griffin, London.

Kleman J, Hättestrand C, Stroeve AP, Jansson KN, De Angelis H, Borgström I. 2006. Reconstruction of Palaeo-Ice Sheets-Inversion of their Glacial Geomorphological Record. *Glacier Sci Environ Chang.*:192–198.

Kotlia BS, Joshi LM. 2013. Late Holocene climatic changes in Garhwal Himalaya. *Curr Sci.*:911–919.

Kulkarni, A.V., Bahuguna, I.M. Rathore, B.P., Singh, S.K., Randhawa, S.S., Sood, R.K. and Dhar S. 2007. Glacial retreat in Himalaya using Indian Remote Sensing satellite data. *Curr Sci.* 92(1):69–74.

Kulkarni, A.V., Rathore, B.P., Mahajan, S. and Mathur P. 2005. Alarming retreat of Parbati glacier, Beas basin, Himachal Pradesh. *Curr Sci.* 88(11):1844–1850.

Kulkarni A V. 1992. Mass balance of Himalayan glaciers using AAR and ELA methods. *J Glaciol.* 38(128):101–104. <https://doi.org/10.1017/S0022143000009631>

Kulkarni A V., Dhar S, Rathore BP, Raj K. BG, Kalia R. 2006. Recession of samudra tapu glacier, chandra river basin, Himachal Pradesh. *J Indian Soc Remote Sens* [Internet]. 34(1):39–46. <https://doi.org/10.1007/BF02990745>

Kumar P, Krishna K. 2021. Temporal fluctuations and frontal changes of Miyar, Takdung and Uldhampu glaciers, Miyar Valley, Himachal Pradesh, India. *Proc Indian Natl Sci Acad.*:1–7.

Mann ME, Zhang Z, Rutherford S, Bradley RS, Hughes MK, Shindell D, Ammann C, Faluvegi G, Ni F. 2009. Global Signatures and Dynamical Origins of the Little Ice Age and Medieval Climate Anomaly. *Science* (80- ) [Internet]. 326(5957):1256–1260. <https://doi.org/10.1126/science.1177303>

Maurer JM, Schaefer JM, Rupper S, Corley A. 2019. Acceleration of ice loss across the Himalayas over the past 40 years. *Sci Adv* [Internet]. 5(6):eaav7266. <https://doi.org/10.1126/sciadv.aav7266>

Mayewski PA, Jeschke PA. 1979. Himalayan and Trans-Himalayan Glacier Fluctuations since AD 1812. *Arct Alp Res* [Internet]. 11(3):267–287. <https://doi.org/10.1080/00040851.1979.12004137>

Mcgrath D, Sass L, O'Neel S, Arendt A, Kienholz C. 2017. Hypsometric control on glacier mass balance sensitivity in Alaska and northwest Canada. *Earth's Futur.* 5(3):324–336.

Mondal A, Lakshmi V, Hashemi H. 2018. Intercomparison of trend analysis of Multisatellite Monthly Precipitation Products and Gauge Measurements for River Basins of India. *J Hydrol.* 565:779–790. <https://doi.org/10.1016/j.jhydrol.2018.08.083>

Nawaz Ali S, Biswas RH, Shukla AD, Juyal N. 2013. Chronology and climatic implications of Late Quaternary glaciations in the Goriganga valley, central Himalaya, India. *Quat Sci Rev* [Internet]. 73:59–76. <https://doi.org/10.1016/j.quascirev.2013.05.016>

Oberoi, L.K., Siddiqui, M.A. and Srivastva D. 2001. Recession pattern of Miyar glacier, Lahul and Spiti district, Himachal Pradesh. *GSI Spec Publ.* 65(2):57–60.

Oerlemans J. 1989. On the response of valley glaciers to climatic change. In: *Glacier fluctuations Clim Chang.* [place unknown]: Springer; p. 353–371.

Owen LA, Bailey RM, Rhodes EJ, Holloway R. 1997. Style and timing of glaciation in the Lahul Himalaya , northern India : a framework for reconstructing late Quaternary palaeoclimatic change in the western Himalayas. *J Quat Sci.* 12(2):83–109.

Owen LA, Benn DI. 2005. Equilibrium-line altitudes of the Last Glacial Maximum for the Himalaya and Tibet: an assessment and evaluation of results. *Quat Int* [Internet]. 138–139:55–78. <https://doi.org/10.1016/j.quaint.2005.02.006>

Owen LA, Derbyshire E, Richardson S, Benn DI, Evans DJA, Mitchell WA. 1996. The quaternary glacial history of the Lahul Himalaya, northern India. *J Quat Sci* [Internet]. 11(1):25–42. [https://doi.org/10.1002/\(SICI\)1099-1417\(199601/02\)11:1<25::AID-JQS209>3.0.CO;2-K](https://doi.org/10.1002/(SICI)1099-1417(199601/02)11:1<25::AID-JQS209>3.0.CO;2-K)

Owen LA, Finkel RC, Barnard PL, Haizhou M, Asahi K, Caffee MW, Derbyshire E. 2005. Climatic and topographic controls on the style and timing of Late Quaternary glaciation throughout Tibet and the Himalaya defined by Be cosmogenic radionuclide surface exposure dating. 24:1391–1411. <https://doi.org/10.1016/j.quascirev.2004.10.014>

Owen LA, Gualtieri LYN, Finkel RC, Caffee MW, Benn DI, Sharma MC. 2001. Cosmogenic radionuclide dating of glacial landforms in the Lahul Himalaya, northern India: defining the

timing of Late Quaternary glaciation. *J Quat Sci.* 16(6):555–563.  
<https://doi.org/10.1002/jqs.621>

Painter TH, Flanner MG, Kaser G, Marzeion B, VanCuren RA, Abdalati W. 2013. End of the Little Ice Age in the Alps forced by industrial black carbon. *Proc Natl Acad Sci.* 110(38):15216–15221.

Pan BT, Zhang GL, Wang J, Cao B, Geng HP, Wang J, Zhang C, Ji YP. 2012. Glacier changes from 1966–2009 in the Gongga Mountains, on the south-eastern margin of the Qinghai-Tibetan Plateau and their climatic forcing. *Cryosph [Internet]*. 6(5):1087–1101.  
<https://doi.org/10.5194/tc-6-1087-2012>

Patel LK, Sharma P, Fathima TN, Thamban M. 2018. Geospatial observations of topographical control over the glacier retreat, Miyar basin, Western Himalaya, India. *Environ Earth Sci [Internet]*. 77(5):190. <https://doi.org/10.1007/s12665-018-7379-5>

Paterson WSB. 2000. *Physics of glaciers*. [place unknown]: Butterworth-Heinemann.

Paul F, Barrand NE, Baumann S, Berthier E, Bolch T, Casey K, Frey H, Joshi SP, Konovalov V, Bris R Le, et al. 2013. On the accuracy of glacier outlines derived from remote-sensing data. *Ann Glaciol [Internet]*. 54(63):171–182. <https://doi.org/10.3189/2013AoG63A296>

Paul F, Kääb A, Maisch M, Kellenberger T, Haeberli W. 2002. The new remote-sensing-derived Swiss glacier inventory: I. Methods. *Ann Glaciol.* 34(1):355–361.  
<https://doi.org/10.3189/172756402781817941>

Paul F, Kääb A, Rott H, Shepherd A, Strozzi T, Volden E. 2009. GlobGlacier : A NEW ESA PROJECT TO MAP THE WORLD ' S GLACIERS AND ICE CAPS FROM SPACE. (9):11–25.

Pettitt AN. 1979. A non-parametric approach to the change-point problem. *J R Stat Soc Ser C (Applied Stat.* 28(2):126–135.

Pfeffer WT, Arendt AA, Bliss A, Bolch T, Cogley JG, Gardner AS, Hagen J-O, Hock R, Kaser G, Kienholz C, et al. 2014. The Randolph Glacier Inventory: a globally complete inventory of glaciers. *J Glaciol* [Internet]. 60(221):537–552. <https://doi.org/10.3189/2014JoG13J176>

Pognante U, Castelli D, Benna P, Genovese G, Oberli F, Meier M, Tonarini S. 1990. The crystalline units of the High Himalayas in the Lahul–Zaskar region (northwest India): metamorphic–tectonic history and geochronology of the collided and imbricated Indian plate. *Geol Mag* [Internet]. 127(02):101. <https://doi.org/10.1017/S0016756800013807>

Prakash S, Sharma MC, Shahnawaz, Pandey VK, Chand P, Deswal S. 2019. Mapping Glacial Geomorphology and Livelihood Resources in Urgos Watershed, Lahul and Spiti District, Himachal Pradesh, India. *J Indian Soc Remote Sens*. 47(8). <https://doi.org/10.1007/s12524-019-01002-9>

Prakash S, Sharma MC, Sreekesh S, Chand P, Pandey VK, Latief SU, Deswal S, Manna I, Das S, Mandal ST, Bahuguna IM. 2021. Decadal terminus position changes and ice thickness measurement of Menthosa Glacier in Lahaul region of North-Western Himalaya. *Geocarto Int* [Internet].:1–20. <https://doi.org/10.1080/10106049.2021.1939437>

Pratap B, Dobhal DP, Mehta M, Bhambri R. 2015. Influence of debris cover and altitude on glacier surface melting : a case study on Dokriani Glacier , central Himalaya , India. 56(70):9–16. <https://doi.org/10.3189/2015AoG70A971>

Racoviteanu AE, Arnaud Y, Williams MW, Manley WF. 2015. Spatial patterns in glacier characteristics and area changes from 1962 to 2006 in the Kanchenjunga–Sikkim area, eastern Himalaya. *Cryosph* [Internet]. 9(2):505–523. <https://doi.org/10.5194/tc-9-505-2015>

Racoviteanu AE, Paul F, Raup B, Jodha S, Khalsa S, Armstrong R. 2009. Challenges and recommendations in mapping of glacier parameters from space : results of the 2008 Global Land Ice Measurements from Space ( GLIMS ) workshop , Boulder , Colorado , USA. 50(53):53–69.

Raina VK. 2009. Himalayan glaciers: a state-of-art review of glacial studies, glacial retreat and climate change. [place unknown].

Raper SCB, Braithwaite RJ. 2006. Low sea level rise projections from mountain glaciers and icecaps under global warming. *Nature*. 439(7074):311–313.

Raper SCB, Braithwaite RJ. 2009. Glacier volume response time and its links to climate and topography based on a conceptual model of glacier hypsometry. *Cryosph*. 3(2):183–194.

Rawat YS, Vishvakarma SCR, Todaria NP. 2009. Fuel wood consumption pattern of tribal communities in cold desert of the Lahaul valley, North-Western Himalaya, India. *Biomass and Bioenergy* [Internet]. 33(11):1547–1557. <https://doi.org/10.1016/j.biombioe.2009.07.019>

Robyr M, Vannay J-C, Epard J-L, Steck A. 2002. Thrusting, extension, and doming during the polyphase tectonometamorphic evolution of the High Himalayan Crystalline Zone in NW India. *J Asian Earth Sci* [Internet]. 21(3):221–239. [https://doi.org/10.1016/S1367-9120\(02\)00039-1](https://doi.org/10.1016/S1367-9120(02)00039-1)

Rowan A V. 2017. The ‘Little Ice Age’ in the Himalaya: A review of glacier advance driven by Northern Hemisphere temperature change. *The Holocene* [Internet]. 27(2):292–308. <https://doi.org/10.1177/0959683616658530>

Saini R, Sharma MC, Deswal S, Barr ID, Kumar P, Kumar P, Kumar P, Chopra S. 2019. Glacio-archaeological evidence of permanent settlements within a glacier end moraine complex during 980-1840 AD: The Miyar Basin, Lahaul Himalaya, India. *Anthropocene*. 26. <https://doi.org/10.1016/j.ancene.2019.100197>

Sarkar A, Ramesh R, Somayajulu BLK, Agnihotri R, Jull AJT, Burr GS. 2000. High resolution Holocene monsoon record from the eastern Arabian Sea. *Earth Planet Sci Lett*. 177(3–4):209–218.

Scherler D, Bookhagen B, Strecker MR, von Blanckenburg F, Rood D. 2010. Timing and extent of late Quaternary glaciation in the western Himalaya constrained by <sup>10</sup>Be moraine

dating in Garhwal, India. *Quat Sci Rev* [Internet]. 29(7–8):815–831.  
<https://doi.org/10.1016/j.quascirev.2009.11.031>

Schmidt, S. and Nusser M. 2012. Changes of High Altitude Glaciers from 1969 to 2010 in the Trans-Himalayan Kang Yatze Massif, Ladakh, Northwest India. *Arctic, Antarct Alp Res*. 44(1):107–121. <https://doi.org/http://dx.doi.org/10.1657/1938-4246-44.1.107>

Sedláček J, Mysak LA. 2009. A model study of the Little Ice Age and beyond: changes in ocean heat content, hydrography and circulation since 1500. *Clim Dyn*. 33(4):461–475.

Sharma M, Owen LA. 1996. Quaternary glacial history of NW Garhwal, Central Himalayas. *Quat Sci Rev*. 15(4):335–365. [https://doi.org/10.1016/0277-3791\(95\)00061-5](https://doi.org/10.1016/0277-3791(95)00061-5)

Shukla A, Gupta RP, Arora MK. 2009. Estimation of debris cover and its temporal variation using optical satellite sensor data: a case study in Chenab basin, Himalaya. *J Glaciol* [Internet]. 55(191):444–452. <https://doi.org/10.3189/002214309788816632>

Singh V, Misra KG, Singh AD, Yadav RR, Yadava AK. 2021. LITTLE ICE AGE REVEALED IN TREE-RING-BASED PRECIPITATION RECORD FROM THE NORTHWEST HIMALAYA, INDIA. *Geophys Res Lett*. <https://doi.org/10.1029/2020GL091298>

Srivastava AK, Rajeevan M, Kshirsagar SR. 2009. Development of a high resolution daily gridded temperature data set (1969-2005) for the Indian region. *Atmos Sci Lett*. 10(4):n/a-n/a. <https://doi.org/10.1002/asl.232>

Taylor PJ, Mitchell WA. 2000. The Quaternary glacial history of the Zaskar Range, north-west Indian Himalaya. *Quat Int* [Internet]. 65–66:81–99. [https://doi.org/10.1016/S1040-6182\(99\)00038-5](https://doi.org/10.1016/S1040-6182(99)00038-5)

Thomas DSG. 2013. Reconstructing paleoenvironments and palaeoclimates in drylands: what can landform analysis contribute? *Earth Surf Process Landforms*. 38(1):3–16.

Vannay J-C, Steck A. 1995. Tectonic evolution of the High Himalaya in Upper Lahul (NW Himalaya, India). *Tectonics* [Internet]. 14(2):253–263. <https://doi.org/10.1029/94TC02455>

Vincent C, Le Meur E, Six D, Funk M. 2005. Solving the paradox of the end of the Little Ice Age in the Alps. *Geophys Res Lett.* 32(9).

Weber P, Andreassen LM, Boston CM, Lovell H, Kvarteig S. 2020. An~ 1899 glacier inventory for Nordland, northern Norway, produced from historical maps. *J Glaciol.* 66(256):259–277.

Wijngaard JB, Klein Tank AMG, Können GP. 2003. Homogeneity of 20th century European daily temperature and precipitation series. *Int J Climatol A J R Meteorol Soc.* 23(6):679–692.

**Table 1: Specification of satellite data used in the study.**

Sensor Type	Scene ID	Acquisition Date	Spatial Resolution (m × m)
Corona Forward	DS1024-1023DF102	24/09/1965	3
Corona Aft	DS1115-2282DA065	28/09/1971	3
Corona Aft	DS1115-2282DA064	28/09/1971	3
KH-9 Hexagon	DZB1216-500361L008001	16/09/1980	7-8
Landsat 5 TM	p147r37_5t19891009	09/10/1989	30
Landsat 7 ETM+	LE71470372011271PFS00	28/09/2002	15, 30
Aster GDEM	ASTGDEM2_0N32E076	17/10/2011	30
Aster GDEM	ASTGDEM2_0N33E076	17/10/2011	30
IRS LISS IV	142673731	23/10/2013	5.6
Landsat 8 ETM+	LC81470372019285LGN00	12/10/2019	15,30

**Table 2: Characteristics of glaciers analyzed in detail in this study.**

Id. no.	Name of glacier	Terminus altitude (m a.s.l.)	Length (km)	Size (km <sup>2</sup> )	ELA (m a.s.l.)	Debris cover (%)	Retreat since LIA (km)	Frontal area loss (km <sup>2</sup> ) since LIA	Retreat Rate (m a <sup>-1</sup> ) since LIA
1.	Miyar	4012	25.8	88.86	5500	19.5	0.9	1.14	5.3
2.	Pimu	4572	4.7	5.52	5090	10.3	2.2	1.13	13
3.	Menthosa	4400	4.3	5.81	5180	24.6	1.6	0.66	9.4
4.	Tharang	4507	4.3	5.37	5500	0.0	2.3	1.03	13.6
5.	Uldhampu	4530	6	4.86	4990	41.3	1.1	0.77	6.5
6.	Neelkanth	4300	7.2	6.27	4940	32.8	1.3	0.75	7.6

**Table 3: Records of terminus retreat (since 1965) for the six valley glaciers selected for detailed investigation in this study, based on Corona, Hexagon, landsat TM, ETM+ and LISS IV satellite images. For each glacier, the total**

terminus retreat (m), and annual average rate of terminus retreat ( $\text{m a}^{-1}$ ) are recorded for various time periods (dictated by the availability of satellite images). Empty cells denote 'data not available'. For each glacier, the total terminus recession over the period of observation (which varies from glacier-to-glacier) is shown in **bold**.

Glacier name	Years	1965-1980	1965-2002	1971-1980	1971-2002	1980-1989	1980-2002	1989-2002	2002-2013	2013-2019	1965-2019	1971-2019	1989-2019
	Year Gap	15	37	9	31	9	22	13	11	6	54	48	30
Miyar	Retreat (m)	116±21				88±48		79±52	77±27	69±27	<b>429±15</b>		
	Rate ( $\text{m a}^{-1}$ )	7.7±1.4				9.8±5.3		6.1±4.0	7.0±2.5	11.5±4.5	<b>7.9±0.3</b>		
Pimu	Retreat (m)			21.6±14.1			232±31		61±27	35±27		<b>349±15</b>	
	Rate ( $\text{m a}^{-1}$ )			2.4±1.5			10.5±1.4		5.5±2.5	5.8±4.5		<b>7.3±0.3</b>	
Menthosa	Retreat (m)		189±29						80±27	97±27	<b>366±15</b>		
	Rate ( $\text{m a}^{-1}$ )		5.1±0.8						7.3±2.5	16.2±4.5	<b>6.8±0.3</b>		
Tharang	Retreat (m)				145±29				323±27	19±7.1		<b>487±15</b>	
	Rate ( $\text{m a}^{-1}$ )				4.7±0.9				29.4±2.5	3.1±1.1		<b>10.1±0.3</b>	

Uldha mpu	Retr eat (m)				503± 29				19±9. 6	24±7. 1		<b>546± 15</b>	
	Rate (m a <sup>-1</sup> )				16.2± 0.9				1.7±0 .8	4±1.1		<b>11.4± 0.3</b>	
Neelk anth	Retr eat (m)							121 ±52	45±9. 6	57±7. 1			<b>223 ±15</b>
	Rate (m a <sup>-1</sup> )							9.3± 4.0	4.1±0 .8	9.5±1 .1			<b>7.4± 0.5</b>

Table 4: Records of area loss since 1965 for the six valley glaciers selected for detailed investigation in this study. For each glacier, the total area loss over the period of observation (which varies from glacier-to-glacier) is shown in **bold**.

		Peri ods	19 65- 19 80	19 65- 20 02	19 71 - 19 80	19 71 - 19 89	197 1- 200 2	19 80- 19 89	198 0- 200 2	19 89- 20 02	200 2- 201 3	20 13- 20 19	196 5- 201 9	197 1- 201 9	198 9- 201 9
		Yea r Gap	15	37	9	18	31	9	22	13	11	6	54	48	30
1	Miya r	Are a loss (m <sup>2</sup> )	99. 23 ± 2.4 8					78. 47 ± 5.2 4		37. 73 ± 4.8 2	37. 54± 2.2 6	43. 35 ± 3.7	<b>296 .32 ± 4.0 5</b>		
		Rat e	6.6 2±					8.7 2±		2.9 0±	3.4 1±	7.2 2±	<b>5.4 8±</b>		

		(m <sup>2</sup> a <sup>-1</sup> )	0.44					0.97		0.22	0.31	0.61	<b>0.11</b>		
2	Pimu	Are a loss (m <sup>2</sup> )			3.02 ± 0.34				103.37 ± 4.86		11.09± 1.66	6.04± 0.9		<b>123.52</b> ± <b>2.64</b>	
		Rat e (m <sup>2</sup> a <sup>-1</sup> )			0.34 ± 0.04				4.70± 0.22		1.01± 0.15	1.0± 0.2		<b>2.57</b> ± <b>0.06</b>	
3	Ment hosa	Are a loss (m <sup>2</sup> )		70.41 ± 2.70							17.97± 3.18	16.53 ± 3.1	<b>104.91</b> ± <b>5.79</b>		
		Rat e (m <sup>2</sup> a <sup>-1</sup> )		1.90± 0.07							1.63± 0.29	2.7± 0.5	<b>1.94</b> ± <b>0.1</b>		
4	Thar ang	Are a loss (m <sup>2</sup> )					47.20± 4.84				146.15 ± 6.70	18.76 ± 3.91		<b>212.11</b> ± <b>4.83</b>	
		Rat e					1.52±				13.29±	3.12±		<b>4.41</b> ±	

		(m <sup>2</sup> a <sup>-1</sup> )					0.16				0.61	0.65		<b>0.1</b>	
5	Uldh amp u	Are a loss (m <sup>2</sup> )					240 .13 ± 7.0 7				2.3 2± 0.7 2	2.9 1± 0.8 6		<b>245 .36 ± 3.7 8</b>	
		Rat e (m <sup>2</sup> a <sup>-1</sup> )					7.7 5± 0.2 3				0.2 1± 0.0 7	0.4 8± 0.1 4		<b>5.1 1± 0.0 7</b>	
6	Neel kant h	Are a loss (m <sup>2</sup> )								40. 01 ± 4.3 2	30. 0± 3.6 3.7 1	31. 17 ± 3.7 1		<b>101 .18 ± 2.8</b>	
		Rat e (m <sup>2</sup> a <sup>-1</sup> )								3.0 ± 0.3 3	2.7 ± 0.3 2	5.1 9± 0.6 1		<b>3.3 7± 0.0 9</b>	

Table 5: topographical details of studied glaciers based on RGI dataset.  $Z_{min}$ ,  $Z_{max}$ ,  $Z_{med}$  and  $Z_{mid}$  are the minimum, maximum, median and mid-point elevation of the glaciers respectively. HI is the hypsometric index.

Glacier	Area	$Z_{min}$	$Z_{max}$	$Z_{med}$	$Z_{mid}$	Slope	Aspect	HI
Miyar	77.618	4017	6236	5142	5126	12.2	204	-1.0
Pimu	5.054	4640	5494	4956	5067	10.9	7	1.7
Menthosa	4.485	4416	6293	4979	5354	17.2	99	2.3
Tharang	6.004	4255	5939	5328	5097	17.9	320	-1.7
Uldhampu	4.672	4524	5895	4905	5209	17.0	322	2.5
Neelkanth	6.394	4267	5982	4749	5124	17.1	19	2.5

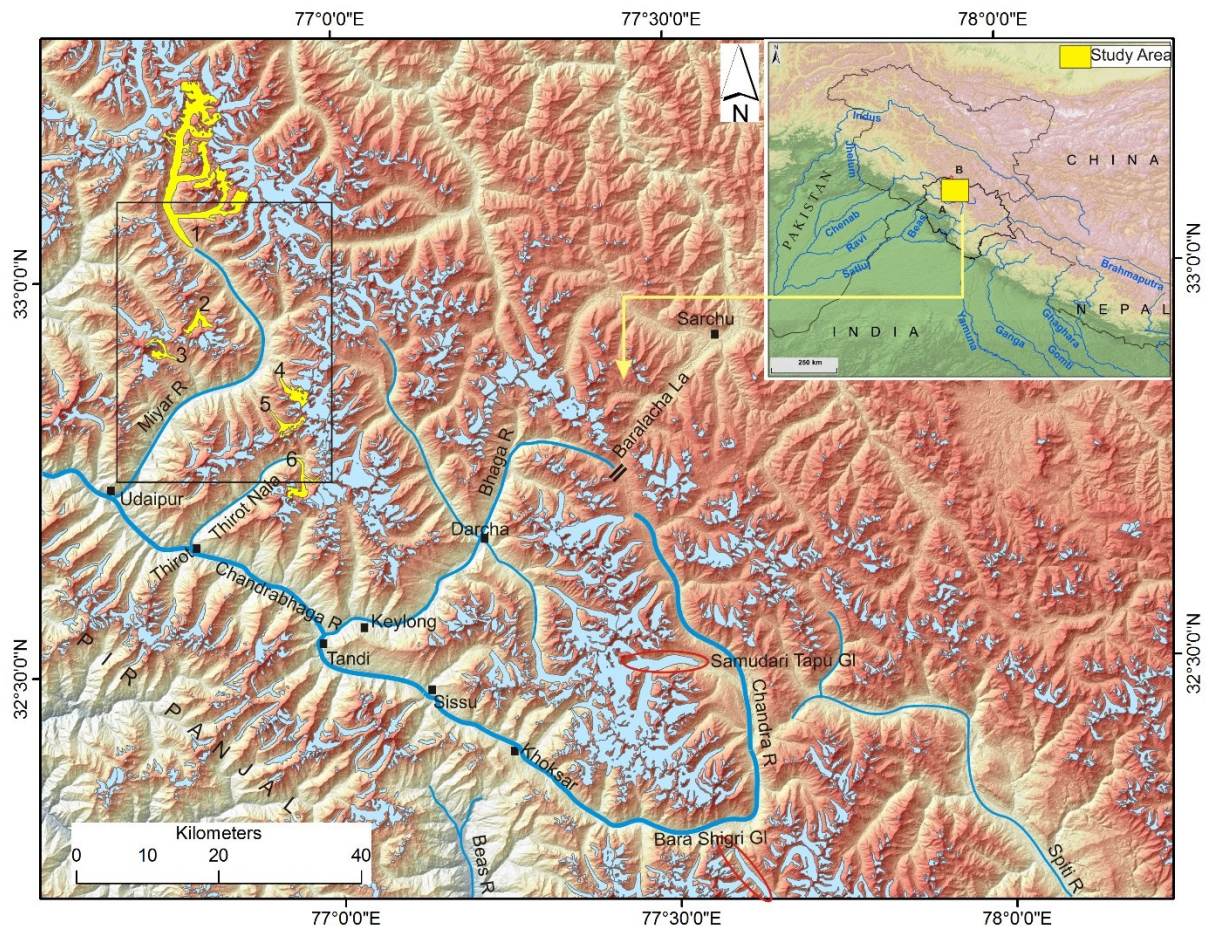


Figure 1: Location map of the study area in the western Himalaya showing the glaciers of the region (RGI V6.0). Studied glaciers are shown in yellow and are numbered as: 1: Miyar, 2: Pimu, 3: Menthosa, 4: Tharang, 5: Uldhampu, and 6: Neelkanth. Rectangle on the left side covers the MTC and shows the location of figure 2(b). ASTER GDEM is used in the background to highlight relief.

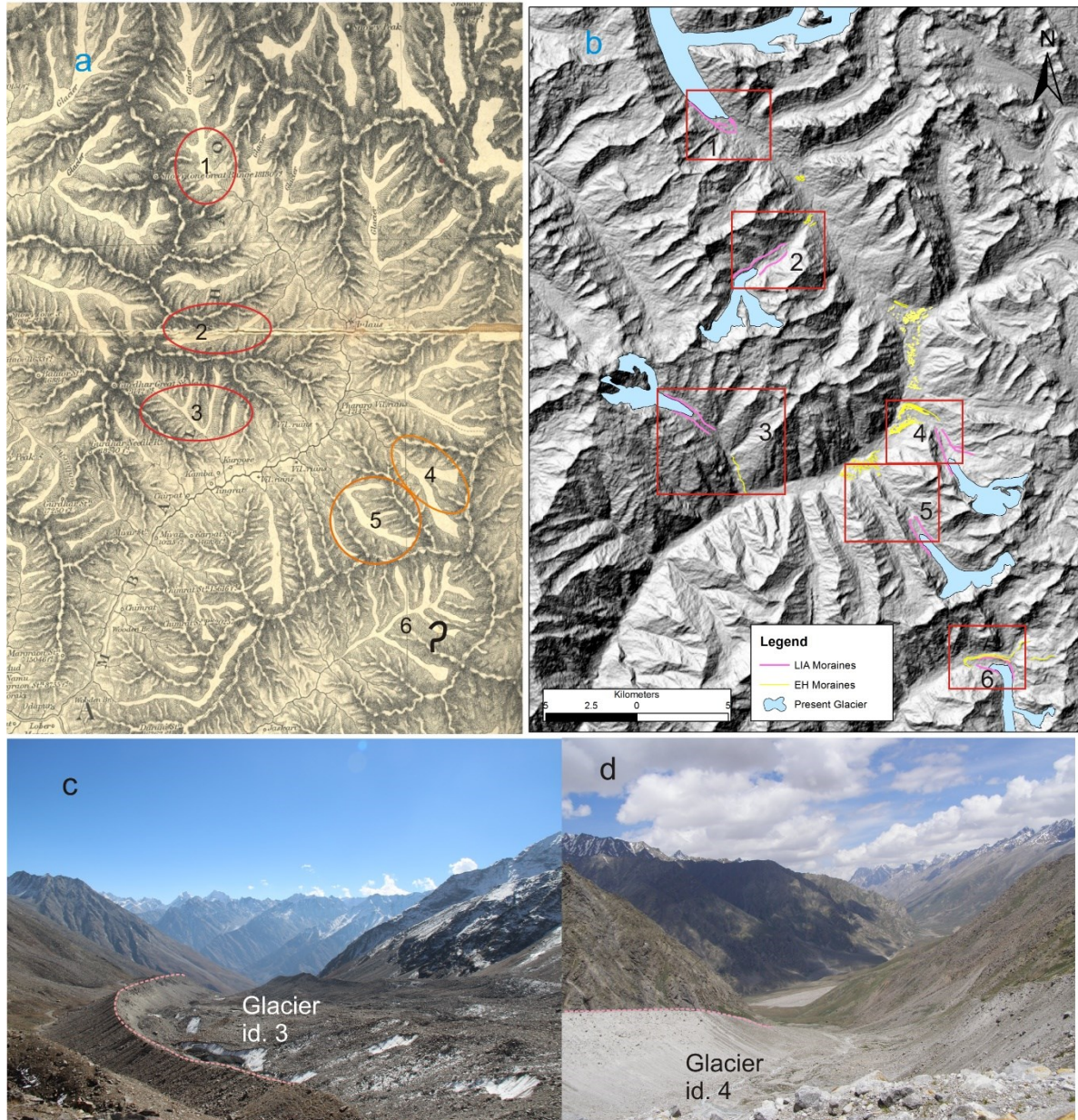


Figure 2: (a) Great trigonometric Survey (GTS) map of 1871 showing the glaciers investigated in this study. Neelkanth glacier (id. 6) is not identifiable in the map. (b) Latero-terminal moraines of studied glaciers (1-6) pertaining to early Holocene (EH) advance and the Little Ice Age (LIA) are shown on ASTER GDEM. (c) & (d) are photographic records of sharp crested LIA lateral moraines of Menthosa & Tharang glaciers (id. 3 & 4) respectively.

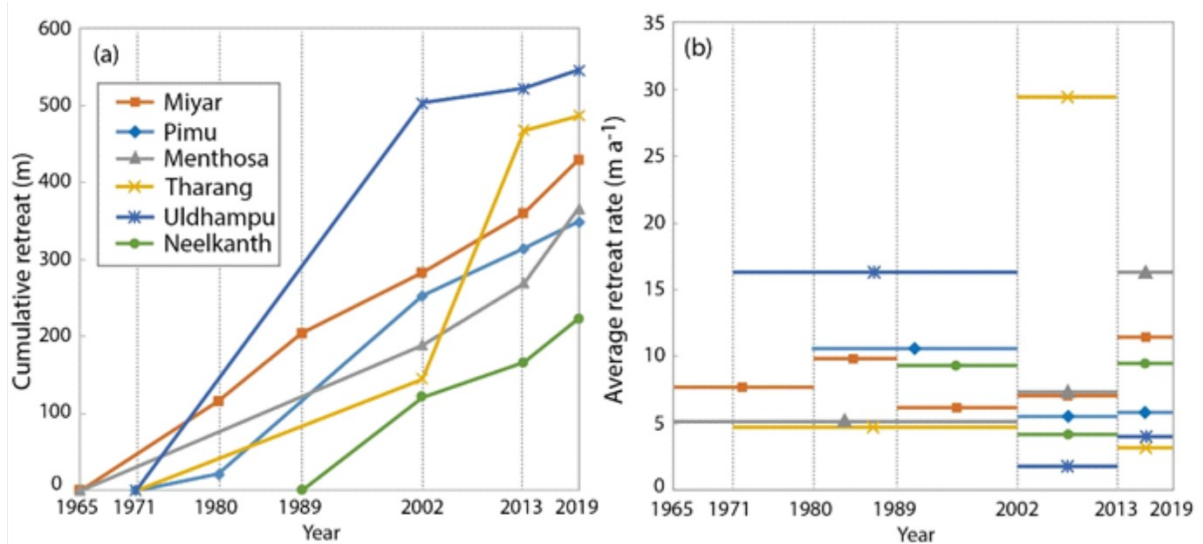


Figure 3: Terminus retreat patterns for the six valley glaciers selected for detailed analysis in this study. (a) Cumulative retreat. (b) Average retreat rates for different time intervals (determined by the availability of satellite imagery).

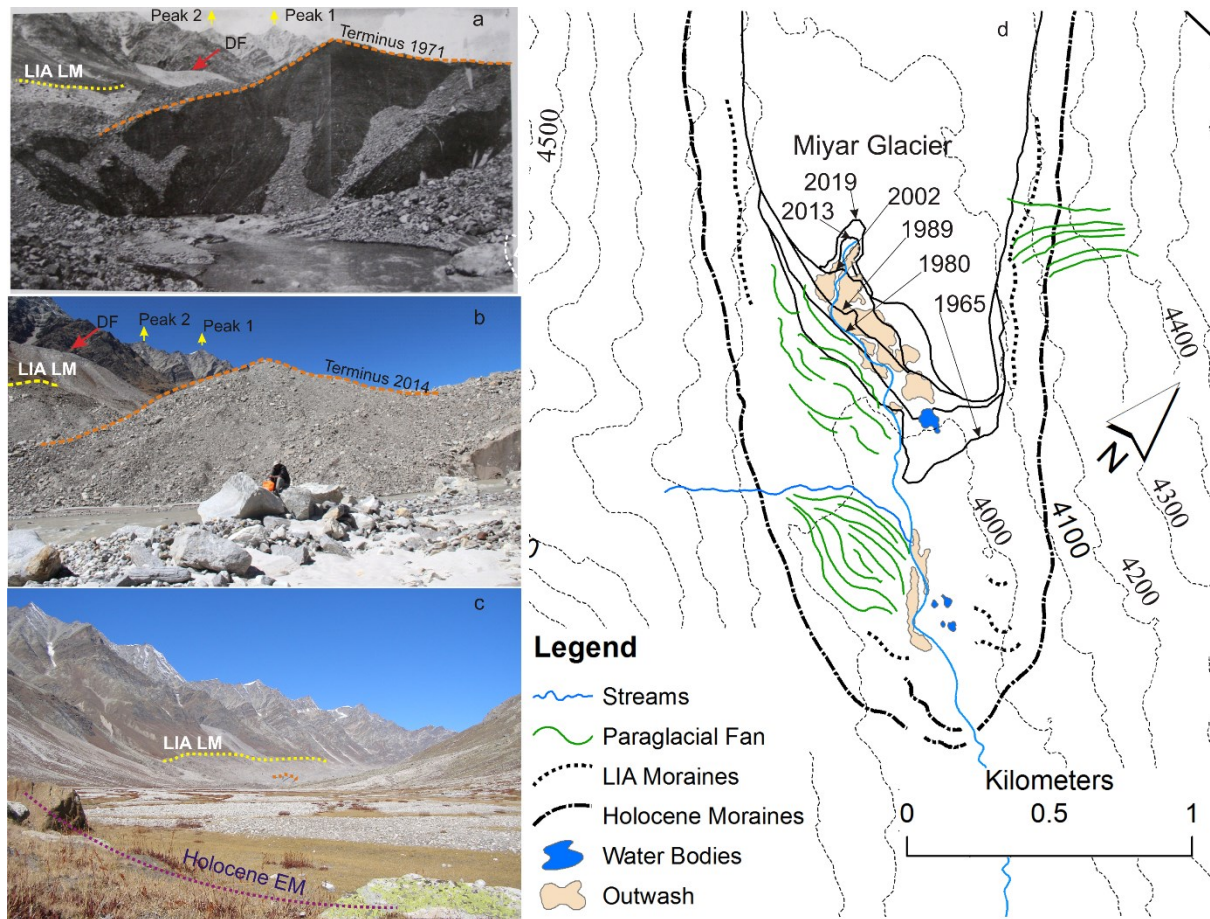


Figure 4: Photographs of Miyar glacier terminus in (a) 1971 (received thankfully from V.K. Raina, Former Deputy Director, Geological Survey of India) and (b) 2014. Visual comparison of DF (debris flow fan) marked by red arrow, shows the recession of the terminus (marked by orange dashed line). (c) Comparative positions of LIA lateral moraines, Holocene end moraine and terminus positions are shown on a field photograph from 2010. (d) Detailed

geomorphological map of Miyar glacier forefield highlighting the relative position of the terminus through the satellite era and latero-terminal moraines pertaining to LIA and Holocene advances.

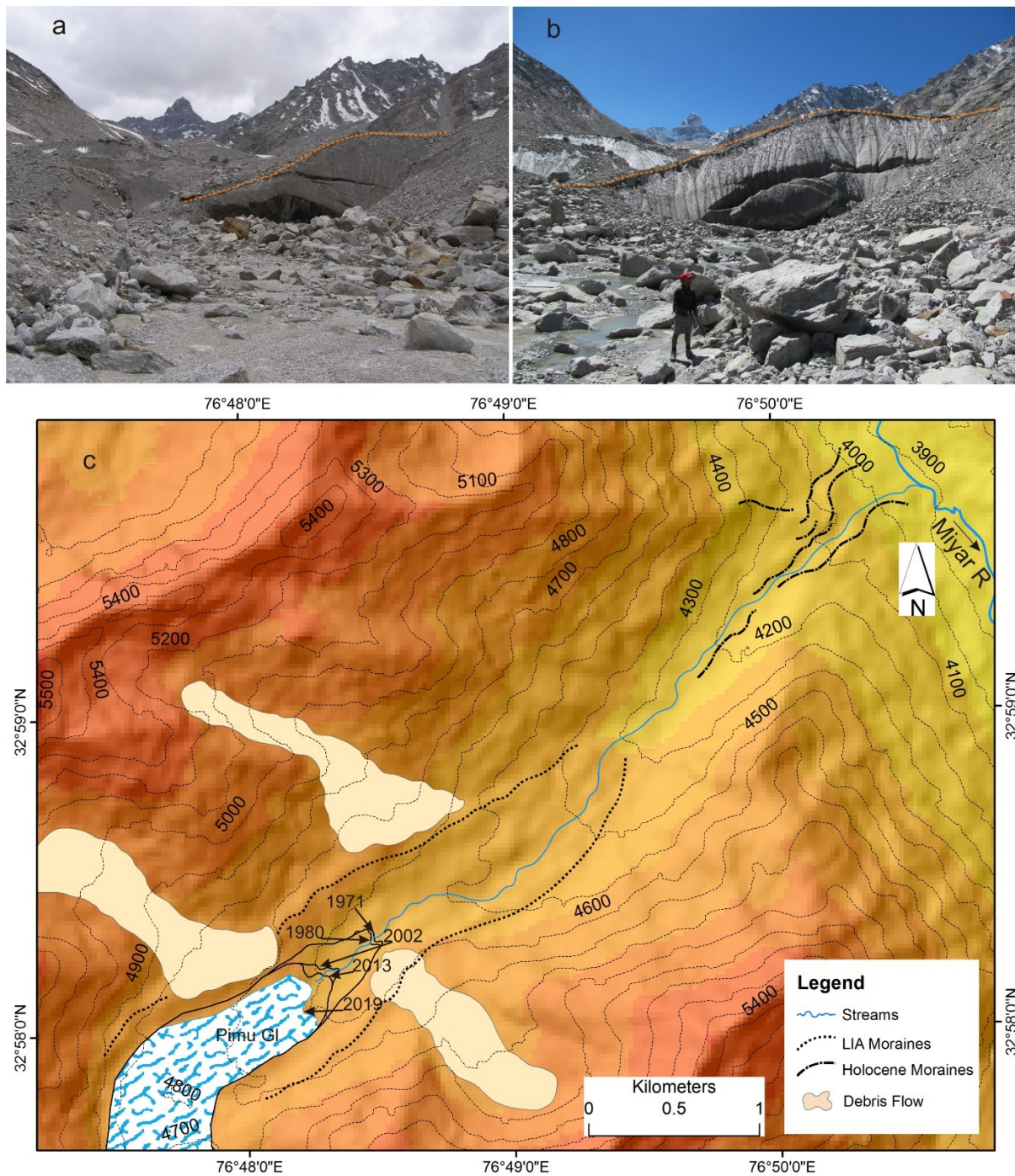


Figure 5: The terminus of Pimu glacier, showing little change between (a) 2008, and (b) 2014. (c) Glacier boundaries during different years and latero-terminal moraines of LIA and the Holocene are shown on the geomorphological map.

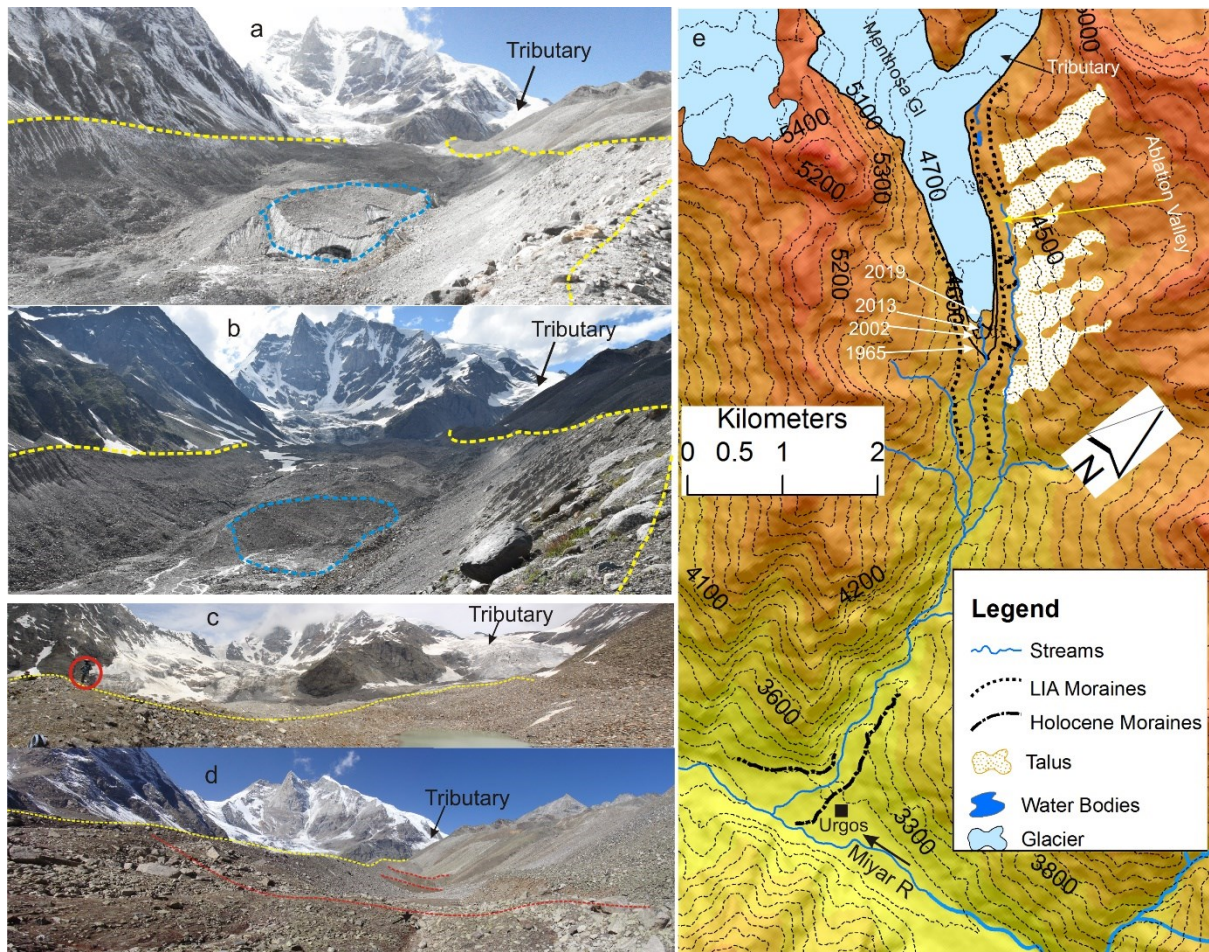


Figure 6: (a) Field photograph from October 2006 and (b) June 2016. The dashed polygon highlights the frontal area loss during this 10-year period. Yellow dashed lines mark the LIA lateral moraines. (c) Photograph showing geomorphological settings of accumulation zone with tributary glacier and LIA moraine marked with yellow dashed line. Human figure is in red circle for scale. (d) Photograph from little down valley side showing the ablation valley with successive older moraines possibly pertaining to the Holocene. (e) Geomorphological map of the Menthosa glacier surroundings highlighting the LIA and Holocene moraines and terminus positions through satellite era.

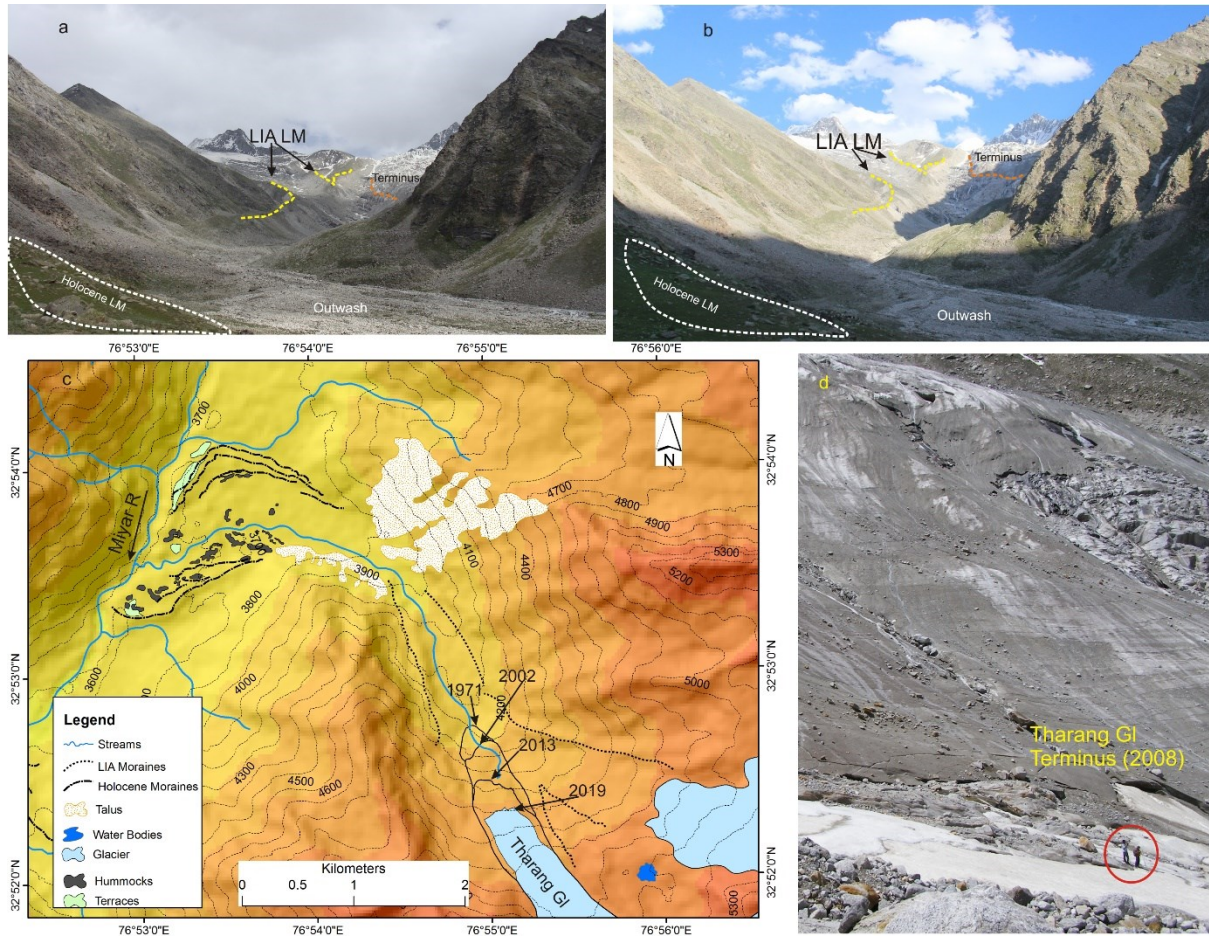


Figure 7: Photographs of Tharang glacier forefield in (a) June 2008 and (b) June 2016. Yellow dashed lines show the LIA lateral moraines. The terminus of the glacier is marked with a orange dashed line, showing change in 8 years. (c) Geomorphological map showing the terminus positions, LIA lateral moraines and the Holocene end-moraine complex. (d) Field photograph of the Tharang glacier terminus highlighting the steep slope of the frontal area. See authors in the red circle for spatial scale.

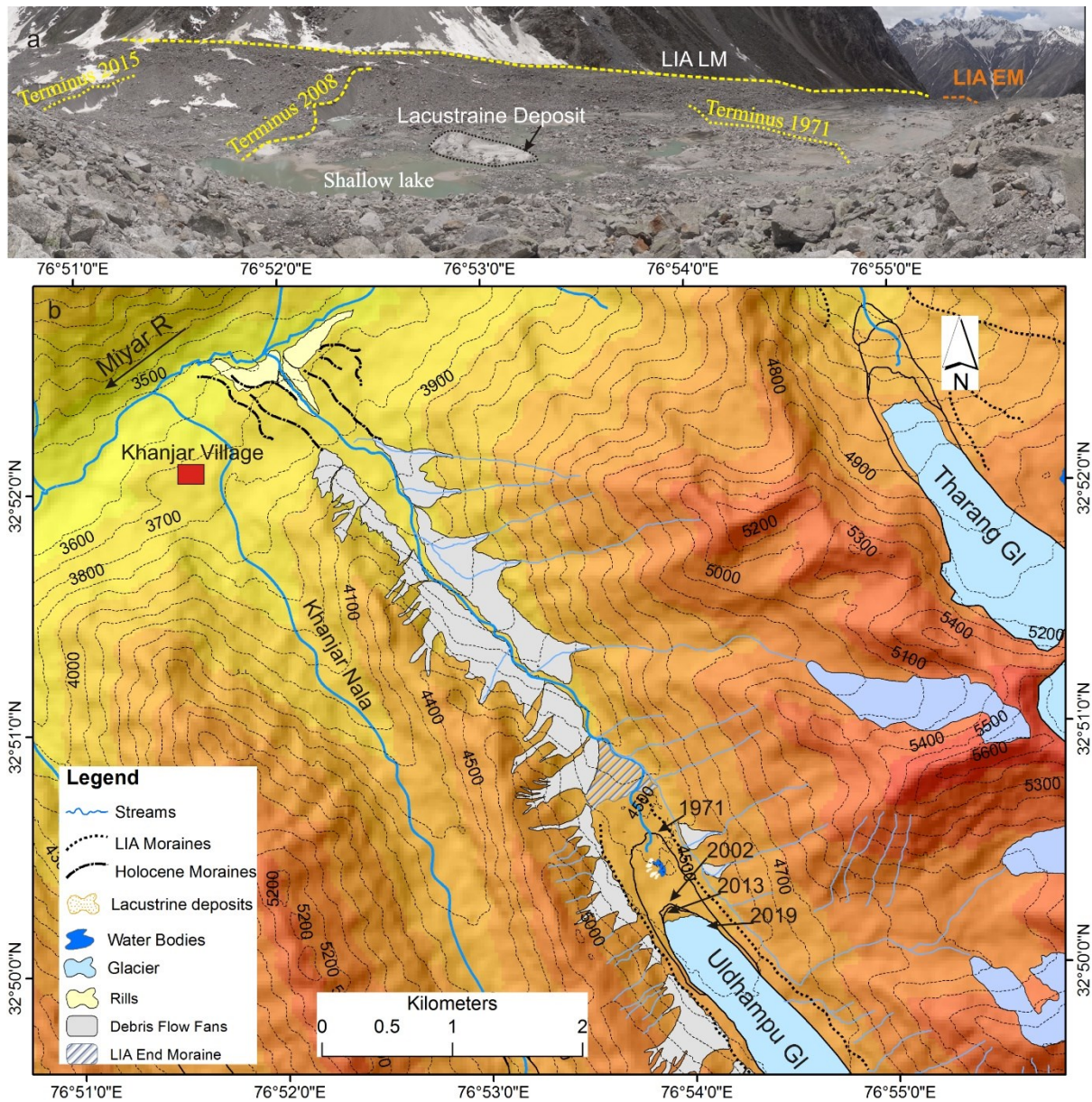


Figure 8: Uldhampu glacier forefield. (a) Field photograph of June 2015 showing the glacier terminus, earlier positions of terminus, LIA lateral Moraine (LM) and LIA end moraine (EM). (b) Geomorphological map illustrating the retreat of Uldhampu glacier's terminus between 1971 and 2019 and the latero-terminal moraines from LIA and the Holocene advances.

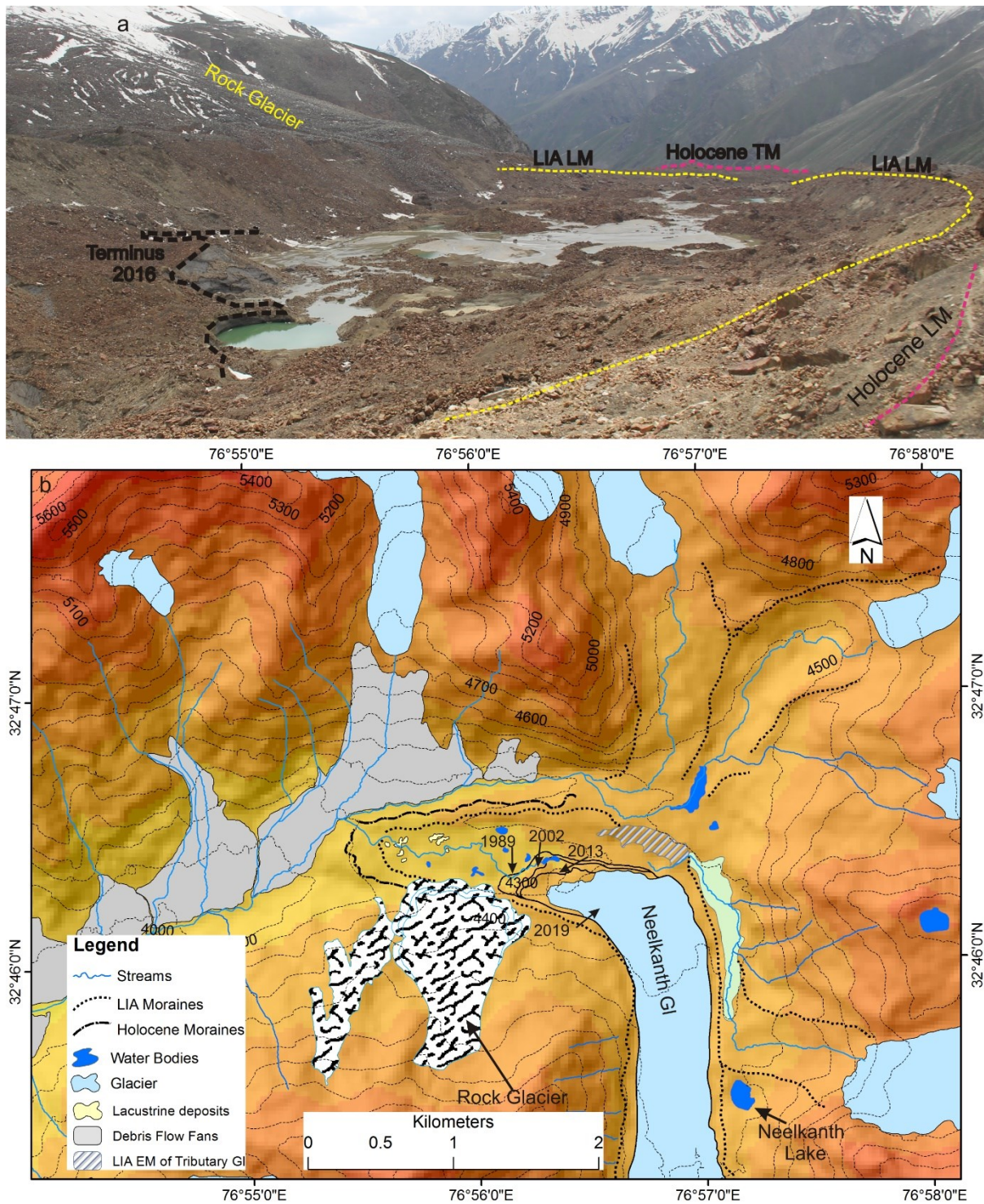


Figure 9: (a) Frontal area of Neelkanth glacier, looking down valley. Moraines belonging to an early Holocene phase and the LIA are marked with dashed lines. (b) Geomorphological map highlighting the peculiarity of this glacier as the LIA advance has nearly approximated the Holocene advance. The terminus position through different periods has also been shown in the map.

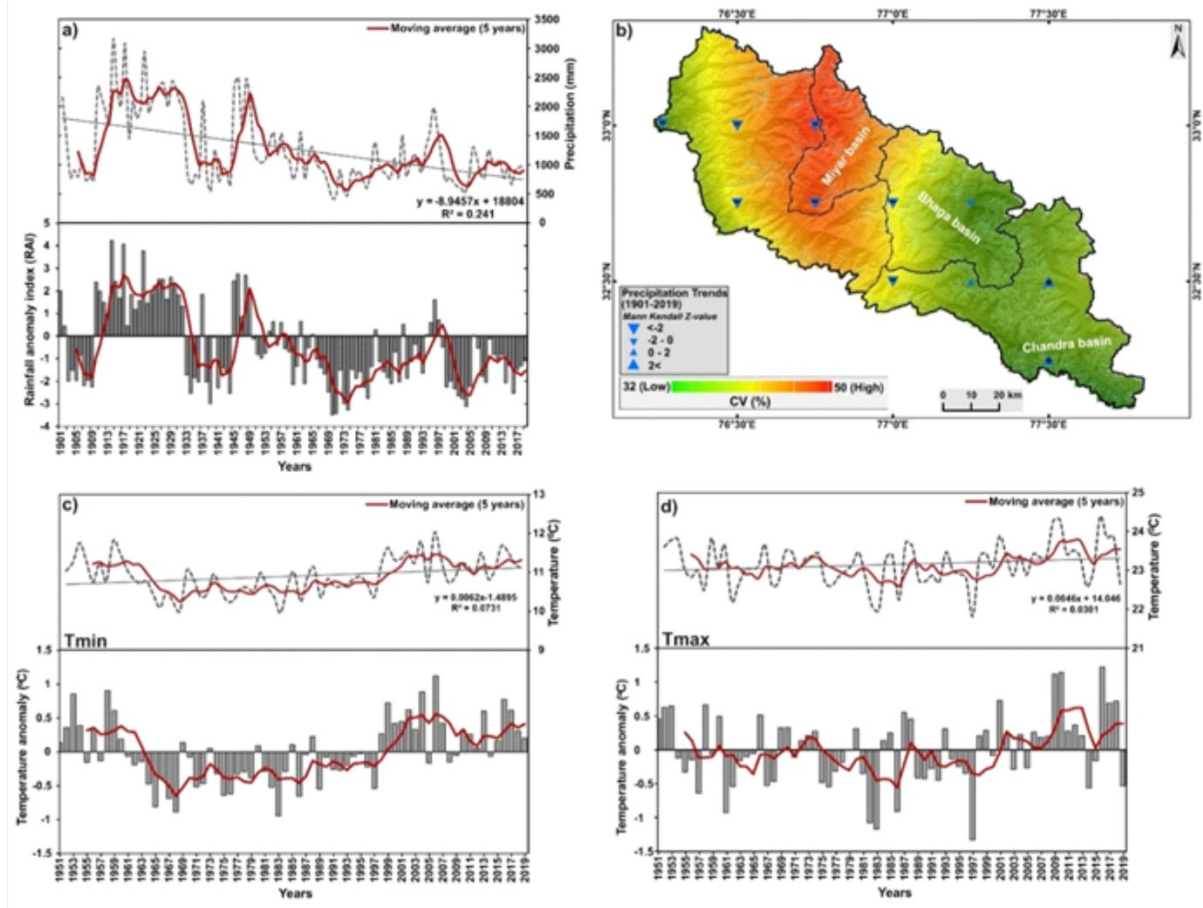


Figure 10: (a) Annual precipitation trend and rainfall anomaly index for the nearest grid cell of the IMD datasets located within the Miyar basin. (b) Interpolated annual variability of precipitation (% CV) during 1901 to 2019. (c) and (d) show temperature anomalies and trends for  $T_{min}$  and  $T_{max}$ , respectively, for the available single grid cell within the Chenab basin from 1951-2019.

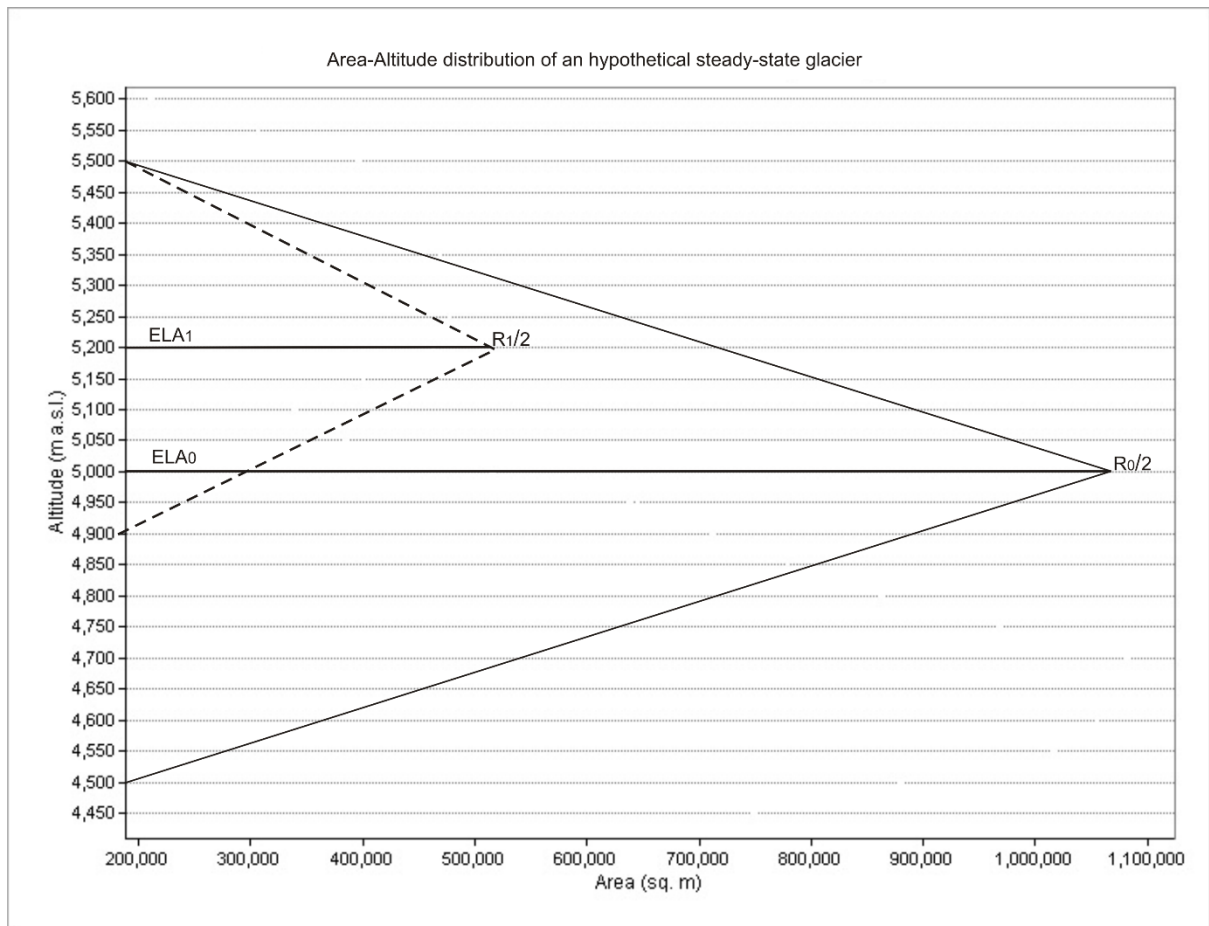


Figure 11: Area-Altitude distribution of a hypothetical steady-state glacier. Note that the mid-point altitude, median altitude and the ELA coincide at the same altitude (adapted and modified from Raper and Braithwaite, 2009).  $ELA_0$  is the initial ELA and  $ELA_1$  is the ELA after climate perturbation. Similarly,  $R_0/2$  is initial half range while  $R_1/2$  is half range after climate perturbation.

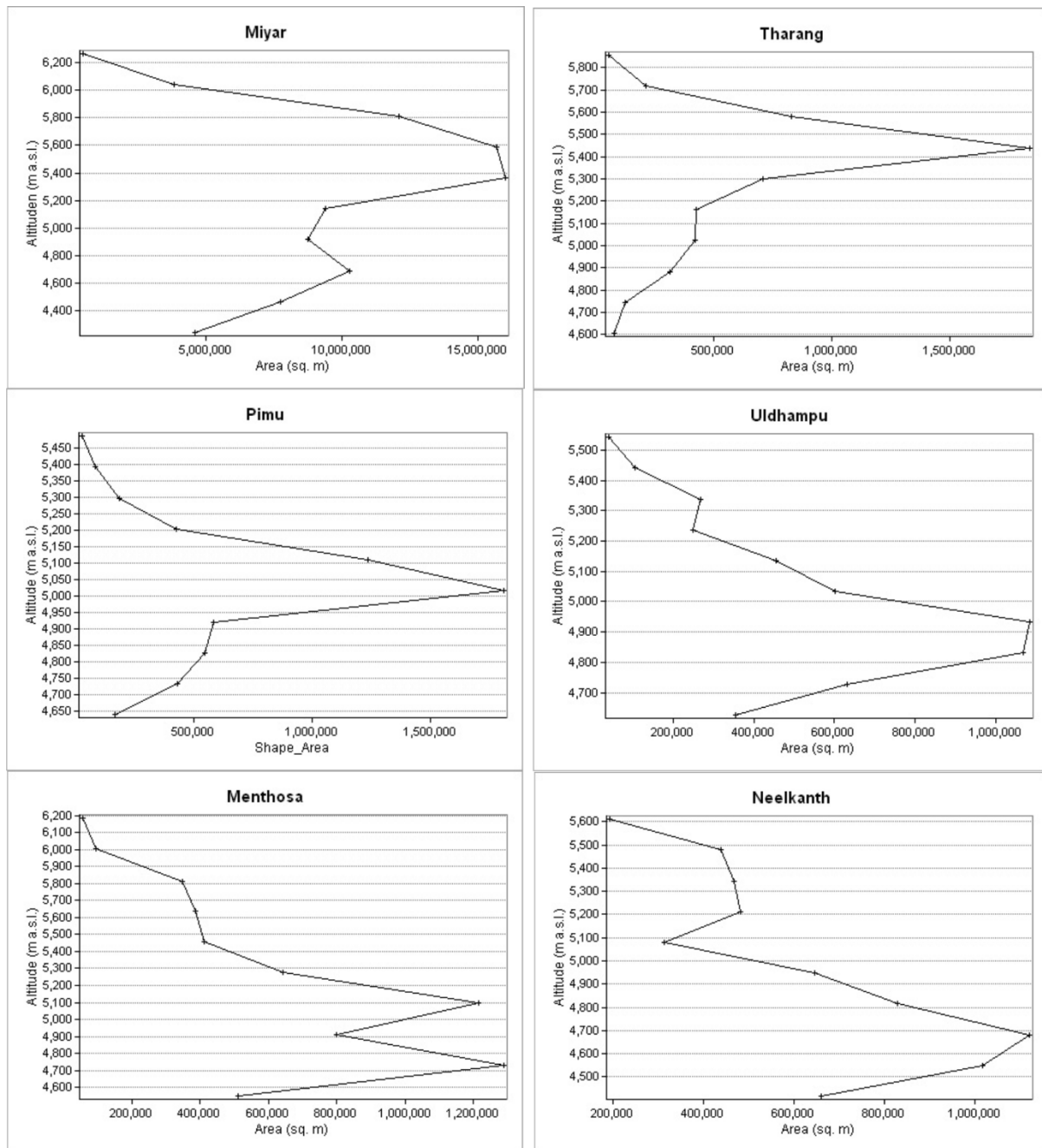


Figure 12: Area-Altitude distribution of the studied glaciers show deviation from ideal steady-state glacier.